UNIVERSIDADE DE LISBOA

FACULDADE DE CIÊNCIAS

DEPARTAMENTO DE QUÍMICA E BIOQUÍMICA

Anoctamins, a novel family of ion channels and their role in intracellular calcium signaling

Inês Maria Santos Cabrita

Dissertação

Mestrado em Bioquímica

Especialização em Bioquímica Médica

Orientação: Prof. Dr. med. Karl Kunzelmann e Prof. Dr. Margarida Ramos

2015

Index

Acknowledgments

For all the success of my thesis work, I would like to show my appreciation to my supervisor, Prof. Karl Kunzelmann, for the unique opportunity of work in a lab that is perfectly organized and successful. For all the orientation, patience and for sharing all his knowledge. I want to express my huge gratitude to Prof. Rainer Schreiber for all the support, orientation, time, motivation, patience and friendship, pointing his big sense of humour. To Prof. Margarida Ramos for all the concern and support along this year.

I also want to recognize the importance of the girls from the lab who made me feel part of a new crazy gang. An endless thanks to Gam, whom biggest heart on earth, covered with princess walls, gave me a huge strength. All the patience, sincerity, compassion and laughs fulfilled me. Her rare bad mood made my mornings happier, like rainbows! A bright future is waiting for her. To Kip, the cutest girl alive, who supported me on everything! For all the giggles, kindness and comfort. She will be the perfect professor. (Kip, you truly are a เจี๊ยบเซ็กซี่!). To Roberta (aka Bernadette) to always have the right friendly word to say. For all the jokes, pranks and ecstasy! She fully supported me in and out of the lab! I am grateful for all the hours, days and nights. *Aspettami*! To Ji, who kept our rambunctious mind in order, for all the knowledge, help and disco nights! With all those dinners, laughs and parties wild… They all made my work easier and my days and nights more joyful. Now seriously, thank you all for wake me up every morning!

A special thanks also goes to our great technical assistants: Patricia, Brigitte and Ernestine, whom help transformed our lab life way easier and cheerful.

Obrigada a todos os meus amigos, cuja amizade ultrapassa os limites. À Ana e ao Nuno, pois sem eles esta aventura não seria possível. Especialmente ao Nuno, por completar cada segundo.

Finalmente, quero expressar todo o meu amor e gratidão a toda a minha família pelo apoio dado. Obrigada ao meu primo Miguel e família por demonstrarem ser possível uma vida científica feliz.

Acima de tudo, o suporte, carinho e incentivo inestimáveis do meu pai, da minha mãe e do meu irmão, nos bons e maus momentos, ajudaram-me e crescer e a amparar esta nova etapa da minha vida. Obrigada por tudo!

I Summary

Ca^{2+} activated TMEM16 Cl^- channels (CaCCs; Anoctamins, ANOs) are anion-selective channels activated by an increase in cytosolic Ca^{2+} concentration. The function of these CaCCs is still unclear, although there are evidences that ANOs could modulate intracellular Ca^{2+} signaling. Recently it was demonstrated that in mouse intestine lacking expression of ANO1, Ca^{2+} dependent Cl^- secretion was significantly reduced. The study also suggested that ANO1 may facilitate Ca^{2+} signaling as a counter ion channel, or as a ER tethering protein or possibly activates the apical CFTR indirectly. ANO6 has been shown to regulate Ca^{2+} signaling indirectly by supporting the activity of the Na^+/Ca^{2+} exchangers (NCX). Moreover, it has been reported that ANO1 interacts with IP_3R, in lipid rafts, tethering the ER, giving new evidences of compartmentalized Ca^{2+} signaling in this membrane compartments.

A recombinant cell system and two animal models were further examined in order to study whether also other proteins of the TMEM16 family change intracellular Ca^{2+} concentration close to the plasma membrane ($[Ca^{2+}]_P$). Therefore, ANO1, -4, -5, -6, -7, -8, -9 and -10 were overexpressed in HeLa cells and ATP-induced changes of $[Ca^{2+}]_P$ were measured, using a plasma membrane targeted calcium sensitive GFP protein. It was observed that overexpression of ANO1, -5 or -10 enhanced, while ANO4, -8, or -9 decreased changes of $[Ca^{2+}]_P$ and that the activity of these proteins is relevant for this regulation. Further studies of cellular localization and co-localization with IP_3 receptors and SERCA pump suggested a localization of ANO1 and ANO4 in different lipid rafts, which could explain the different effect on changes of $[Ca^{2+}]_P$. For ANO10 the effects on Ca^{2+} signaling were confirmed in murine renal proximal tubules and intestinal epithelial knockout cells.

This study describes innovative evidences for a new role of anoctamins in intracellular Ca^{2+} signaling. It is suggested that anoctamins may regulate a compartmentalized Ca^{2+} signaling in different lipid rafts or simply act as counter ion channels, which may give a hint to the wide cellular functions of anoctamins. broader

Key words: Anoctamin, Ca^{2+} signaling, PM-GCaMP2, Endoplasmic Reticulum, Calcium activated Chloride Channels (CaCCs).

II Resumo

A sinalização de cálcio é um mecanismo ubíquo, responsável pela regulação de vários processos fisiológicos celulares, mas também pela comunicação entre células. Destes estão incluídos transcrição, regulação do ciclo celular, diferenciação, motilidade/migração celular, apoptose, contração/relaxamento muscular, fertilização e excitabilidade neuronal. De forma a fazer uso de tal sinal, as células necessitam de estar equipadas com diversas ferramentas sofisticadas para regular precisamente estes sinais de cálcio.

A concentração de cálcio intracelular ronda os 100 nM sendo que os níveis extracelulares são de 2 mM. Este nível intracelular pode aumentar até mais do que 1 μM após as células serem estimuladas, por exemplo, por ativação hormonal (como por exemplo por adenosina trifosfato – ATP). Este aumento de $[Ca^{2+}]_i$ é responsável por uma versátil sinalização de cálcio, portanto é importante compreender o mecanismo pelo qual as células procedem à sua regulação.

Os canais de cloreto ativados pelo cálcio (do inglês *Calcium Activated Chloride Channels* – CaCCs) são canais aniónicos seletivos que são ativados pelo aumento de concentrações citosólicas de cálcio. Os CaCCs participam em múltiplas funções fisiológicas, entre as quais: secreção de electrólitos/fluídos, excitabilidade do músculo liso, repolarização e duração de potencial de ação nos neurónios, estabilização de potencial de membrana nos fotorreceptores e fertilização em oócitos. Em 2008 a proteína TMEM16A (ANO1, Anoctamina 1) foi caracterizada como sendo um CaCC e pertence a uma família de proteínas transmembranares constituída por 10 membros (TMEM16A-K ou ANO1-10), que apresentam semelhança estrutural: dez segmentos transmembranares, um poro e cujos terminais amina e carboxilo se encontram localizados na face citoplasmática da membrana plasmática ou vesícula.

A função das anoctaminas é ainda incerta, mas existem evidências de que estas proteínas estão envolvidas na sinalização intracelular de Ca^{2+}. Recentemente foi demonstrado que, em intestino de murganhos *knockout* para a ANO1, a secreção de Cl^- dependente de Ca^{2+} é significativamente reduzida. Também foram sugeridos três mecanismos pelos quais a ANO1 facilita a sinalização de Ca^{2+}: ou funcionando como um *counter ion channel* – onde, ao transportar Cl^-, mantém a neutralidade

elétrica da célula; ou ativando os canais K^+ dependentes de Ca^{2+}, facilitando a secreção de Cl^- dependente do *Cystic Fibrosis Transmembrane Conductance Regulator* (CFTR); ou possibilitando a ativação apical do canal CFTR através da inibição de fosfatases dependentes de Ca^{2+} e/ou ativando a Proteína Cinase C (PKC). Para além disso, noutro estudo foi também demonstrado que a ANO1 interage, nas jangadas lipídicas da membrana plasmática, com o receptor de inositol trifosfato (IP_3R) do retículo endoplasmático, resultando num *tethering* entre estes dois componentes celulares, o que revelou novas evidências de uma sinalização compartimentalizada de Ca^{2+} nestes domínios membranares. Curiosamente a proteína de levedura IST2, que é caracterizada como sendo um homólogo das anoctaminas, é uma proteína importante para o *tethering* que detém a membrana plasmática em conjunto com o retículo endoplasmático, mantendo junções entre estes dois compartimentos. A IST2 é localizada na membrana do retículo e demonstra um alto nível de homologia com a ANO10.

Foram também apresentadas fortes evidências de que, em osteoblastos, a ANO6 permite a entrada de Ca^{2+} e regula a sua sinalização indiretamente ao potenciar a atividade dos canais antiporte de Na^+/Ca^{2+} (NCX).

Estas evidências prévias de regulação da sinalização de Ca^{2+} dependente da ANO1 e da ANO6 permitiram uma melhor compreensão deste mecanismo de sinalização, porém, é necessário um conhecimento mais detalhado sobre esta regulação.

O trabalho elaborado teve como objetivo estudar num sistema celular recombinante e em dois modelos animais se também outras proteínas da família TMEM16 alteram a concentração intracelular de Ca^{2+} ($[Ca^{2+}]_i$) ou próxima da membrana plasmática ($[Ca^{2+}]_P$). O âmbito do trabalho visava a regulação de células epiteliais, onde a ANO1, -4, -5, -6, -7, -8, -9 e -10 são expressas, sendo que ANO2 e a ANO3 não foram estudadas porque são maioritariamente expressas em neurónios. Deste modo, a ANO1, -4, -5, -6, -7, -8, -9 ou -10 foram sobreexpressas em células HeLa e as alterações da $[Ca^{2+}]_i$ induzidas por ATP foram medidas, utilizando o indicador de Ca^{2+} fluorescente Fura-2 AM. Este indicador dá informação sobre alterações da $[Ca^{2+}]_i$ após um estímulo, onde é possível obter um pico inicial, que representa a libertação de Ca^{2+} armazenado no retículo endoplasmático e um posterior plateau que representa o influxo de Ca^{2+} celular. Foi assim possível estudar as consequências da sobreexpressão destas ANOs na regulação destes processos de sinalização de cálcio. Para cada um destes processos de sinalização foi possível

distinguir as ANOs em dois grupos. A sobreexpressão da ANO5 ou da ANO6 aumenta a libertação de Ca^{2+} armazenado no retículo endoplasmático, enquanto a da ANO4 diminui esta libertação. O influxo celular de Ca^{2+} é inibido pela sobreexpressão da ANO4, -6, -8 ou -9 e ativado pela sobreexpressão da ANO5. A sobreexpressão da ANO1, da ANO7 e da ANO10 não suscitou nenhuma alteração significativa em termos de alterações de $[Ca^{2+}]_i$.

Quando uma variante da proteína GFP sensível ao cálcio expressa na membrana plasmática (PM-GCaMP2) foi co-expressa com as diferentes ANOs mencionadas anteriormente, foi possível medir alterações específicas da $[Ca^{2+}]_P$. Este novo indicador revela um sinal transiente que representa a libertação de Ca^{2+} armazenado no retículo endoplasmático quando induzida por ATP. Foi possível dividir os elementos da família TMEM16 estudados em dois grupos: a sobreexpressão da ANO1, -5 ou -10 leva a um aumento da $[Ca^{2+}]_P$, enquanto que a sobreexpressão ANO4, -8, ou -9 a diminui. Não foi possível porém, observar alterações da $[Ca^{2+}]_P$ dependentes da sobreexpressão da ANO6 e da ANO7.

A utilização de inibidores específicos para anoctaminas, como Ácido Niflúmico (NFA) e CaCC-AO1, demonstrou que a atividade destas proteínas é necessária para esta regulação. Estudos da ANO6 e da ANO10 endógenas nestas células demonstraram que estas proteínas são necessárias para as alterações de Ca^{2+} induzidas por ATP, anteriormente observadas.

Foram realizados estudos adicionais de localização celular e co-localização destas proteínas com recetores de IP_3 e a bomba SERCA de forma a perceber como diferenças na localização subcelular levam a diferentes alterações da $[Ca^{2+}]_P$. Quando sobreexpressas, a ANO1 e a ANO6 localizam-se na membrana plasmática das células HeLa, enquanto a ANO4, -5, -7, -8, -9 e -10 foram observadas nas membranas de outros organelos celulares.

Graças aos estudos de imunocitoquímica e utilizando um polieno antibiótico, Filipina, que se associa ao colesterol, levando à destabilização das jangadas lipídicas, foi observado que a ANO1 e a ANO4 são expressas em diferentes localizações celulares. Quando estes domínios transmembranares foram destabilizados, observou-se um aumento da sinalização de cálcio, tanto quando a ANO1 ou a ANO4 foram sobreexpressas, tendo-se obtido um sinal não específico, e concluiu-se que o indicador PM-GCaMP2 é expresso nas jangadas lipídicas da membrana plasmática.

A sobreexpressão da ANO1 demonstrou uma co-localização desta proteína com o recetor de IP_3 e resultou numa distribuição deste até à membrana plasmática, corroborando as evidências de que esta anoctamina é responsável por um *tethering* do retículo plasmático à membrana, aumentando a $[Ca^{2+}]_P$ em compartimentos de jangadas lipídicas. Observou-se também que a ANO4 co-localiza-se com a bomba SERCA, noutros compartimentos celulares, diminuindo a $[Ca^{2+}]_P$.

Finalmente foi realizado o estudo em dois modelos animais que não expressam a ANO10 em túbulos proximais do rim ou em criptas do jejuno intestinal, de forma a perceber como esta proteína endogenamente expressa regula a sinalização de Ca^{2+}. As alterações de $[Ca^{2+}]_i$ induzidas por ATP foram medidas com o indicador Fura-2 AM e comparadas com murganhos *wild-type* (wt). Observou-se que a ANO10 potencia a sinalização de Ca^{2+} nestes dois tipos de células epiteliais, sendo que os efeitos na sinalização de Ca^{2+} anteriormente observados foram corroborados.

Concluindo, neste trabalho são discutidas evidências inovadoras de uma nova função das anoctaminas na sinalização de cálcio. É sugerido que estas proteínas estão envolvidas na regulação de uma sinalização de Ca^{2+} compartimentalizada em jangadas lipídicas, resultante do *tethering* retículo endoplasmático–membrana plasmática, ou simplesmente envolvidas na regulação de sinalização de Ca^{2+} como *counter ion channels*, elucidando assim, as amplas funções celulares das anoctaminas.

Key words: Anoctamina (ANO), sinalização de Ca^{2+}, PM-GCaMP2, Retículo Endoplasmático, Canais de Cloro ativados pelo Cálcio (CaCCs).

III Abbreviations

λ	Wavelength
[Ca^{2+}]	Ca^{2+} concentration
[Ca^{2+}]$_i$	Intracellular free Ca^{2+} concentration
[Ca^{2+}]$_P$	Ca^{2+} concentration near to the Plasma Membrane
%	Percentage
ANO	Anoctamin
ANOVA	Analysis of variance
ATP	Adenosine Triphosphate
BSA	Bovine Serum Albumin
Ca^{2+}	Calcium ion
CaCC	Calcium-activated Chloride Channel
CAM	Calcium-modulated Protein
CaM	Calmodulin
Cav-1	Caveolin-1
CCH	Carbachol
CD8	Cluster of Differentiation 8
cDNA	Complementary DNA
CFP	Cyan Fluorescent Protein
CFTR	Cystic Fibrosis Transmembrane Conductance Regulator
Cl^-	Chloride ion
cm	Centimetre
CO_2	Carbon Dioxide
COOH-terminal	Carboxyl-terminal
cpEGFP	Circularly permuted eGFP
DAG	Diacylglycerol
DAPI	4´,6-diamidino-2-phenylindole
DF	Dilution Factor
DMEM	Dulbecco's Modified Eagle's
DMSO	Dimethyl Sulfoxide
DTT	Dithiothreitol
eGFP	Enhanced Green Fluorescent Protein

EGTA	Ethylene Glycol Tetraacetic Acid
ER	Endoplasmic Reticulum
FBS	Fetal Bovine Serum
g	Gram
GAPDH	Glyceraldehyde 3-phosphate dehydrogenase
GFP	Green Fluorescent Protein
GPCR	G Protein-coupled Receptor
Gq	Gq heterotrimeric G protein
h	Hour
HBSS	Hank's Balanced Salt Solution
HeLa	Henrietta Lacks Cervical Carcinoma *cell line*
Indo	Indometracin
IP_3	Inositol-1,4,5-triphosphate
IP_3R	Inositol-1,4,5-triphosphate receptor
K^+	Potassium ion
kb	Kilobase (1000 base pairs)
Kd	Dissociation constant
KO	Knockout
L	Litter
M	Molar
M13	M13 fragment of myosin light chain kinase
mg	Milligram
Mg^{2+}	Magnesium ion
min	Minute
mL	Millilitre (10^{-3} L)
MLCC20	First 20 amino acids of neuromodulin
mm	Millimetre (10^{-3} m)
mM	Millimolar (10^{-3} M)
NCX	Na^+/Ca^{2+}-exchangers
NFA	Niflumic Acid
ng	Nanogram (10^{-9} g)
NH_2-terminal	Amino-terminal
nM	Nanomolar (10^{-9} M)

nm	Nanometre (10^{-9} m)
O/N	Overnight
ºC	Degree Celsius
Orai1	Calcium release-activated Ca^{2+} channel protein 1
ORCC	Outwardly Rectifying Chloride Channel
P2Y	Purinergic G Protein-coupled Receptor
PBS	Phosphate Buffer Saline
PCR	Polymerase Chain Reaction
PFA	Paraformaldehyde
PIP_2	Phosphatidyl Inositol-4,5-diphospate
PKC	Protein Kinase C
PLC	Phospholipase C
PM	Plasma Membrane
PM-GCaMP2	Plasma Membrane targeted Ca^{2+} sensitive GFP protein
PMCA	Plasma Membrane Ca^{2+} ATPase
PS	Penicillin-Streptomycin
PT	Proximal Tubules
R	Fluorescence ration observed with Fura-2 AM
R_{max}	Maximum fluorescence at saturating [Ca^{2+}]
R_{min}	Minimum fluorescence in the absence of Ca^{2+}
ROCC	Receptor-Operated Ca^{2+} channel
rpm	Rotations per minute
RT	Room temperature
RT-PCR	Reverse Transcription Polymerase Chain Reaction
RyR	Ryanodine Receptor
SDS	Sodium Dodecyl Sulfate
sec	Second
SEM	Standard Error of the Mean value
SERCA	Sarco-endoplasmic Reticulum Ca^{2+} ATPase
Sf_2/Sb_2	Ratio of fluorescence of free and Ca^{2+}-bound Fura-2 measured at 380 nm
siRNA	Small interfering RNA
SOCC	Store-Operated Ca^{2+} channel

SOCE	Store-operated Ca^{2+} Influx
SR	Sarcoplasmic Reticulum
STIM1	Stromal-interacting Molecule 1
TMD	Transmembrane Domains
TMEM16	Transmembrane protein 16
Tris	Tris-(hidroxymethyl)aminoethane
TRP	Transient Receptor Potential
UV	Ultraviolet (light)
v/v	Volume/Volume
VGCC	Voltage-gated Ca^{2+} Channel
VOCC	Voltage-Operated Ca^{2+} channel
w/v	Weight/Volume
wt	Wild-type
µg	Microgram (10^{-6} g)
µL	Microliter (10^{-6} L)
µM	Micromolar (10^{-6} M)

1. Introduction

1.1 Calcium signaling

Intracellular calcium signaling is a ubiquitous toolkit responsible for regulating several features of physiological processes within cells, but also communication between them. Those include for example, transcription, cell cycle regulation, differentiation, cell motility/migration, apoptotic cell death, muscle contraction/relaxation, fertilization and neuronal excitability[1]. In order to make use of such an apparently simple signal, cells need to be equipped with a sophisticated machinery to precisely regulate different calcium (Ca^{2+}) signals in a widely localization-specific and time-dependant manner.

Cells have an intracellular Ca^{2+} concentration ($[Ca^{2+}]_i$) of ~100 nM, and an extracellular level around 2 mM. However, stimulation of cells, for example by depolarisation, mechanical deformation or hormonal activation, causes an increase of cytosolic $[Ca^{2+}]$ to level of 1 µM or more[1]. This calcium increase is responsible for the versatile regulation of calcium signaling; therefore, it is important to understand the mechanisms by which cells regulate Ca^{2+} concentrations.

1.1.1 Calcium signaling toolkit

The Ca^{2+} signaling toolkit is composed of a large amount of components distributed into main functional units (Fig. 1). The signaling is triggered with a stimulus, which generates Ca^{2+}-mobilizing signals, with an internal and external source of Ca^{2+}. Inositol-1,4,5-triphosphate receptor (IP_3R) and ryanodine receptor (RyR) are well known to be the responsible channels of Ca^{2+} release from the internal stores of the endoplasmic reticulum (ER) or the equivalent organelle from muscle cells, sarcoplasmic reticulum (SR). RyR is activated by Ca^{2+} entry through PM, a process called Ca^{2+}-induced Ca^{2+} release and the IP_3R is activated by inositol-1,4,5-triphosphate (IP_3)[2].

When an agonist binds to a G protein-coupled receptor (GPCR), like ATP to a purinergic G protein-coupled receptor ($P2Y_2$), the α-subunit of the Gq heterotrimeric G protein (Gq) can bind to a phospholipase C (PLC) which is activated, resulting in

the cleavage of phosphatidyl inositol-diphospate (PIP_2) into IP_3 and diacylglycerol (DAG). IP_3R, recognizes IP_3, which triggers the opening of the Ca^{2+} channel, and thus release Ca^{2+} into the cytoplasm[3] (Fig. 1).

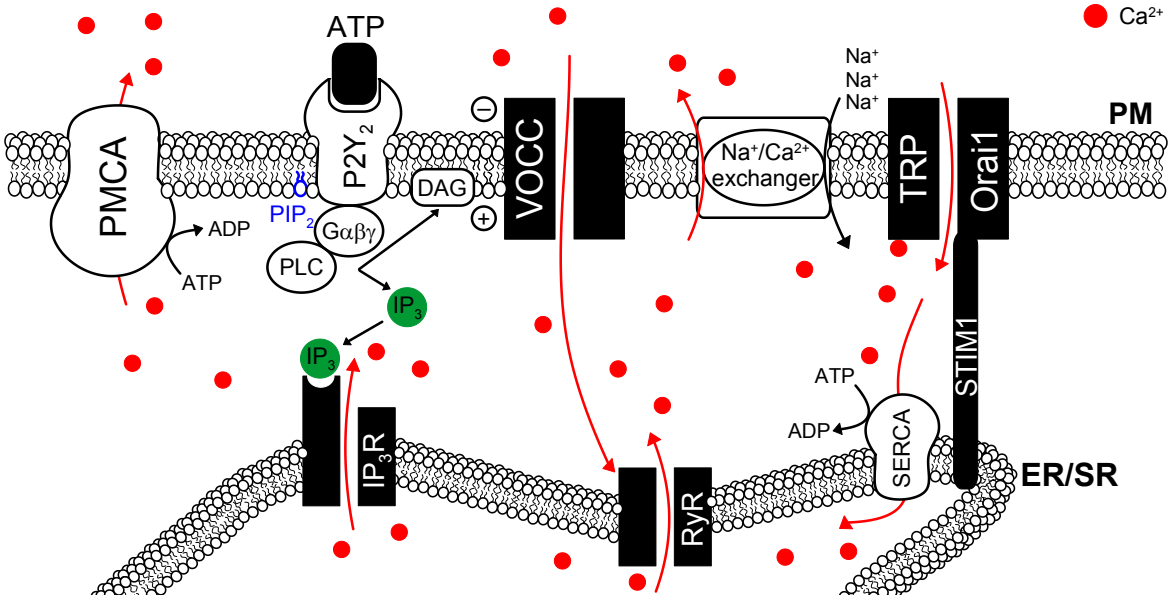

Figure 1. Elements of the Ca^{2+} signaling toolkit. Cells have an extensive signaling toolkit, examples are here represented. The ON mechanisms include a variety of cell-surface receptors, like G-protein (G)-liked $P2Y_2$ receptors, PM Ca^{2+} channels – which respond to membrane depolarization (ΔV) – and intracellular Ca^{2+} channels in the ER/SR, the IP_3 receptor (IP_3R) and ryanodine receptor (RyR). The RyR is activated by a process called Ca^{2+}-induced Ca^{2+} release. The IP_3R is stimulated by inositol-1,4,5-trisphosphate (IP_3), which is generated by activation of $P2Y_2$ receptors by ATP. Phospholipase C (PLC) is activated through G-proteins and hydrolysed phosphatidyl inositol-4,5-diphosphate (PIP_2) to diacylglycerol (DAG) and inositol-1,4,5-triphosphate (IP_3). The IP_3 induced store release of Ca^{2+} causes a drop of the ER Ca^{2+} concentration, which is sensed by STIM1. STIM1 interact with ORAI1 or TRP channel and induces Ca^{2+} entry. The OFF mechanisms pump Ca^{2+} out of the cytoplasm: the Na^+/Ca^{2+} exchanger and the plasma membrane Ca^{2+} ATPase (PMCA) pumps Ca^{2+} out of the cell and the sarco-endoplasmic reticulum Ca^{2+} ATPase (SERCA) pumps it back into the ER/SR.

Nevertheless, there are several different types of Ca^{2+} influx channels on the PM responsible to provide Ca^{2+} to the cytoplasm. The presence of receptor-operated (ROCC), voltage-operated (VOCC) and store-operated (SOCC) Ca^{2+} channels allows the entry of Ca^{2+} ions from the extracellular space (Ca^{2+} influx), resulting in an increase of intracellular calcium concentrations ($[Ca^{2+}]_i$)[1].

Store-operated Ca^{2+} influx (SOCE) is involved in several physiological processes, within the depletion of Ca^{2+} stores activate Ca^{2+} channels in the plasma membrane (like Calcium release-activated calcium channel protein 1 (Orai1) or transient receptor potential (TRP)). Orai1 interacts with stromal-interacting molecule 1 (STIM1), which is a ER Ca^{2+} sensor, leading to a facilitated Ca^{2+} uptake to the ER.

The depletion of luminal ER Ca^{2+} signals, in a retrograde fashion to the plasma membrane, leads to the activation of SOCE[4].

Finally, once the Ca^{2+} has carried out its signaling functions, the OFF mechanism is activated. This mechanism is composed by pumps and exchangers, which remove Ca^{2+} from the cytoplasm to restore the resting state. The Na^{+}/Ca^{2+} exchanger and the plasma membrane Ca^{2+} ATPase (PMCA) pump Ca^{2+} out of the cell and the sarco-endoplasmic reticulum Ca^{2+} ATPase (SERCA) pumps it back into the internal stores[5,6] (Fig. 1).

1.2 Calcium signaling and Anoctamins

1.2.1 Calcium-activated Chloride Channels

Calcium activated Chloride Channels (CaCCs) are anion-selective channels activated by cytosolic Ca^{2+} increase and can be found in several cell types (like neurons; various epithelial cells; olfactory and photo-receptors; cardiac, smooth, and skeletal muscle cells[7], although with slight differences regarding their biophysical properties and pharmacology[7,8]. CaCCs play several roles in many cellular functions, including epithelial secretion[9-13], sensory transduction and adaptation[14], regulation of smooth muscle contraction[15], control of neuronal and cardiac membrane excitability[16-18], oocyte fertilization[19], nociception[20], among others[21-25].

The activation of CaCCs depends on cytosolic Ca^{2+}, from either Ca^{2+} influx or Ca^{2+} release from intracellular stores, in a range of 0.2-5 μM[7]. Experimentally the activation can be elicited by stimulating cells with Ca^{2+}-mobilizing agonists (like adenosine triphosphate – ATP), Ca^{2+} ionophores (such as ionomycin), Ca^{2+}-containing pipette solutions loading or by adding Ca^{2+} to the bath in excised inside-out patches[21].

These channels are also characterized by the halide selectivity of $SCN^{-} > NO3^{-} > I^{-} > Br^{-} > Cl^{-} > F^{-}$, whereas the highly permeable ions influence the channel activation, accelerating it, and slowing down the deactivation[7].

1.2.2 Anoctamins

Anoctamins are a family of Ca^{2+} activated Cl^{-} channels comprised of ten homologous proteins Anoctamin 1-10 (TMEM16A-K; ANO1-10). These proteins are ubiquitously expressed in nearly every cell type and play an essential role in volume regulation,

epithelial Cl^- secretion, neuronal excitability, and also nociception[26]. Mutations in anoctamin proteins lead to various diseases including bone and muscle dystrophy, cerebellar ataxias, and blood coagulation defect[27]. Also, up-regulation of anoctamins is highly linked to different types of cancers[27]. This family of proteins was identified as a family of CaCCs but their precise function is still under examination. Since the discovery of ANO1 in 2008, as a Ca^{2+} activated Cl^- channel[22-24], the protein was found to fulfil various physiological functions in many different type of tissues.

Anoctamins are comprised of 800-1,000 amino acid residues[27] and a X-ray structure of the TMEM16 homologue, nhTMEM16 from *Nectria haematococca* showed a structure consisting of ten putative transmembrane domains (TMD), a pore loop and the NH_2- and COOH termini protruding into the cytosol (Fig. 2)[28]. The overall structural homology within the putative pore region is considerable, but the overall structure within this family remains unclear[26,28].

ANO1 and 2 are reported to be CaCCs[22-24], ANO6 operates as an essential component of the outwardly rectifying chloride channel (ORCC), while others were reported as intracellular proteins.

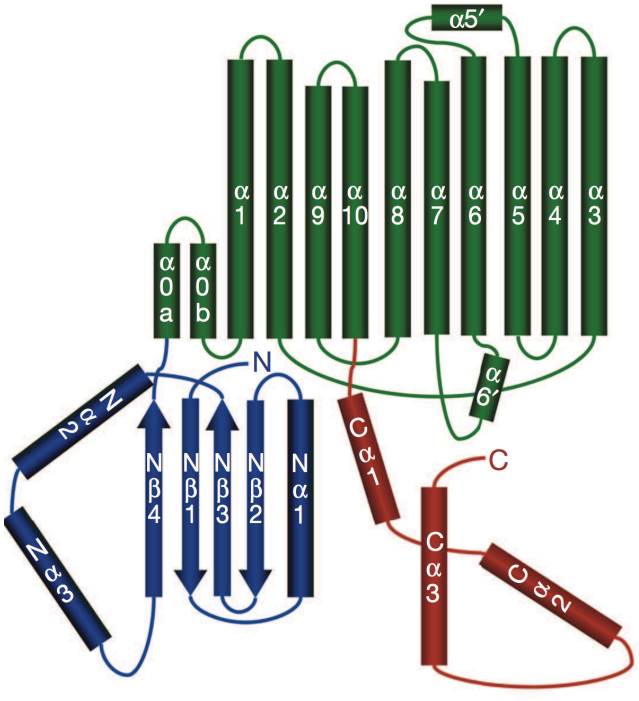

Figure 2. Model for TMEM16 homologue, nhTMEM16 from *Nectria haematococca*, indicating ten transmembrane α-helices (green), a pore loop, and the NH_2- and COOH termini protruding into the cytosol (blue and red, respectively). Retrieved from Brunner *et al.*, 2014[28].

1.2.3 ANO1 and intestinal Ca^{2+}-dependent Cl^- secretion

Intestinal epithelium secretes Cl^- transiently upon stimulation with carbachol, histamine, and nucleotides[29-31]. These agonists increase $[Ca^{2+}]_i$, which leads to activation of CaCCs and triggers a secretory response. Thus although the presence

of CaCC in intestinal epithelium is well established, its significance remains to be resolved.

Last year, Schreiber *et al.* examined whether ANO1 is an independent secretory Cl^- channel or whether it operates in conjunction with cystic fibrosis transmembrane conductance regulator (CFTR), as previous work had suggested. It was shown that in mouse colon, ANO1 is expressed in, or close to the basolateral membrane[32].

With Fura-2 AM measurements of isolated intestinal crypts, it was shown that basolateral ANO1 supports CCH-induced Ca^{2+} signaling since when lacking ANO1, calcium store release and calcium influx were significantly reduced.

All together, these data indicated that ANO1 supports mouse intestinal Cl^- secretion by CFTR, the only apical exit pathway for Ca^{2+}-activated Cl^- secretion.

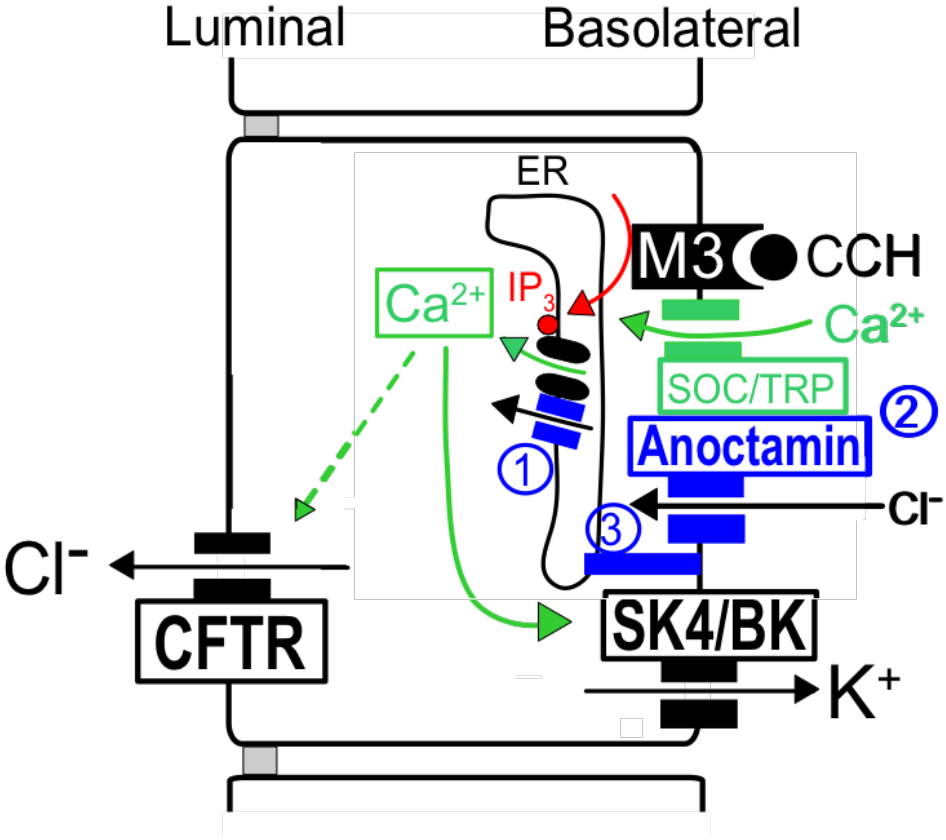

Figure 3. Basolateral ANO1 supports intestinal Cl^- secretion. Transport model for intestinal Ca^{2+}-activated Cl^- secretion: **(1)** Basolateral ANO1 may be localized in the endoplasmic reticulum (ER) and facilitate Ca^{2+} release by IP3 receptors, as a counter ion channel; **(2)** Ca^{2+} influx may be controlled by ANO1 either indirectly by supporting Ca^{2+} store emptying or again, as Cl^- bypass channel; **(3)** ANO1 could tether basolateral ER to the plasma membrane (PM) and thereby facilitate activation of basolateral Ca^{2+}-activated K^+ channels. Retrieved and edited from Schreiber *et al.*, 2014[32].

It was also presented a transport model for intestinal Ca^{2+}-activated Cl^- secretion[32], showing three possible mechanisms for ANOs regulation (Fig. 3):

(1) Basolateral ANO1 may be localized in the endoplasmic reticulum (ER) and facilitate Ca^{2+} release by IP_3R, as a counter ion channel;
(2) ANO1 can control Ca^{2+} influx either indirectly by supporting Ca^{2+} store emptying or again, as a Cl^- bypass channel;
(3) ANO1 may tether basolateral ER to the plasma membrane (PM) and thereby facilitate the activation of basolateral Ca^{2+}-activated K^+ channels, supplying an additional driving force for apical Cl^- secretion by CFTR, moreover activating CFTR through inhibition of phosphatases and increase of protein kinase C activity.

1.2.4 ANO6 and Ca^{2+} entry in osteoblasts

ANO6 allows Ca^{2+} entry[33] and regulates Ca^{2+} signaling indirectly by supporting the activity of the Na^+/Ca^{2+} exchangers (NCX), which explains the defect in bone mineralization detected in ANO6 knockout animals[34]. Ousingsawat *et al.* demonstrated that Cl^- channel function of ANO6 serves to activate NCX1 and possibly NCX3, thereby increasing extracellular Ca^{2+} deposition, required for the formation of hydroxyapatite in the extracellular matrix. It was shown that NCX1 is a potential binding partner of ANO6 with a molecular and functional interaction that efficiently translocates Ca^{2+} out of osteoblasts into the calcifying bone matrix (Fig. 4)[34].

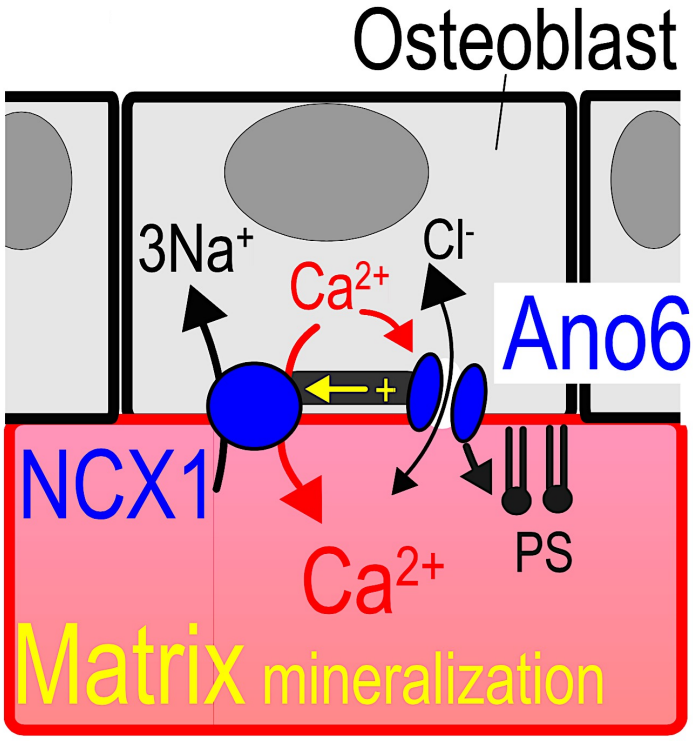

Figure 4. ANO6 regulates Ca^{2+} signaling indirectly by supporting the activity of NCX1 in bone mineralization. Schematic model of the roles of ANO6 and NCX1. Na^+/Ca^{2+} exchanger 1 (NCX1) and ANO6 interaction (yellow arrow) and scrambling of phosphatidylserine (PS) by ANO6. Retrieved from Ousingsawat *et al.*, 2015.

Ca^{2+} increase in osteoblasts activates outwardly rectifying ANO6 Cl^- currents and the outward transport of Ca^{2+} by the Na^+/Ca^{2+} exchanger NCX1. Inward transport of Cl^- compensates the cytosolic positive transport potential by the electrogenic Na^+/Ca^{2+} exchanger, thereby maintaining Ca^{2+} outward transport at a high rate. Therefore, NCX1 may directly interact with ANO6 and this anoctamin is responsible scrambling of phosphatidylserine (PS), which supports the mineralization process (Fig. 4).

1.2.5 Anoctamins as Tethering proteins

The yeast protein IST2, an anoctamin homologue, was found as an important tethering protein that holds plasma and ER membranes together to maintain plasma membrane–ER junctions[35,36]. IST2 is localized in the ER membrane extending its C-terminus to the cytosol. A poly-basic domain at the very end of the IST2 C-terminus acts as an anchor that attaches to the plasma membrane to form a junction with the ER.

Between all the anoctamins, ANO10 shows the highest degree of homology to this IST2 protein.

Jin *et al.* indicated stimulating findings for the role of ANO1 in small nociceptive dorsal root ganglia neurons, as a part of a signaling complex that also harbours G-protein coupled receptors (GPCRs)[37]. They reported that ANO1 is selectively activated by GPCR-induced release of Ca^{2+} from ER stores, but not by Ca^{2+} influx through voltage-gated Ca^{2+} channels. Such a specific Ca^{2+} signaling is accomplished by ANO1/IP_3R interaction, where lipid rafts (PM domains) express ANO1 and are tethering juxtamembrane regions of the ER (Fig. 5).

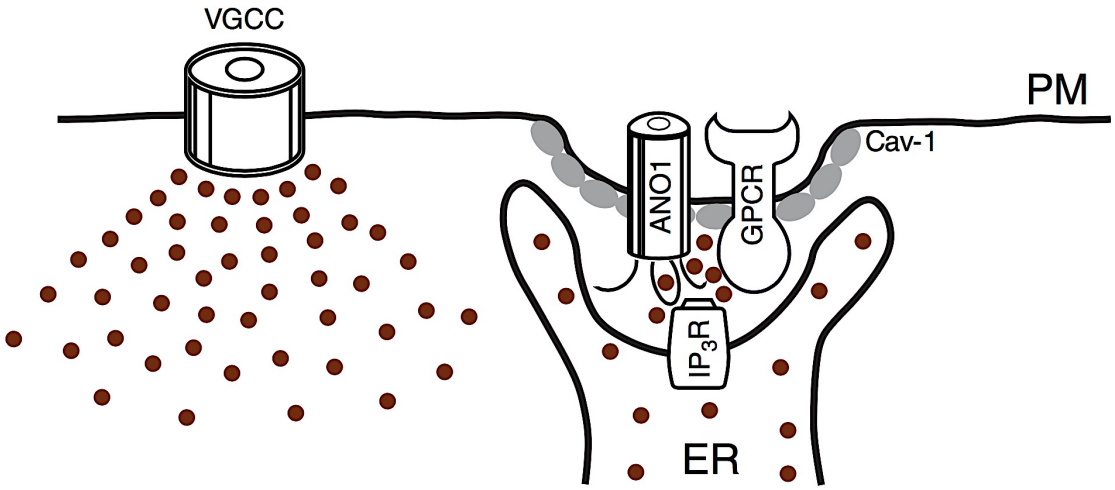

Figure 5. Simplified schematic diagram of the proposed juxtamembrane arrangements within an ANO1-containing signaling microdomain in a nociceptive sensory neuron. Co-assembly of ANO1, GPCR and IP3 receptors. ANO1, anoctamin-1; Cav-1, caveolin-1; ER, endoplasmic reticulum; GPCR, G protein-coupled receptor; IP_3R, inositol-1,4,5-trisphosphate receptor; PM, plasma membrane; VGCC, voltage-gated Ca^{2+} channels; brown circles represent Ca^{2+} ions. Retrieved from Jin *et al.*, 2014[37].

Moreover, ANO1 was found to interact with ERLIN1 (SPFH1), a protein expressed in the ER and lipid rafts, that associates dynamically with IP_3R, further corroborating the role of ANO1 in Ca^{2+} signaling[38]. This compartmentalized Ca^{2+} signaling enables ANO1-mediated excitation in ganglia neurons, rather than the global $[Ca^{2+}]_i$[37], giving a whole new complexity to Ca^{2+} signaling and ANO1 role.

These reports of ANO1 and ANO6 regulation allowed a better understanding of calcium signaling mechanism. However, are these proteins the only players in Ca^{2+} signaling, or are also other members of this novel family involved? More detailed knowledge about its regulation is needed.

1.3 PM-GCaMP2

A novel fluorescent indicator of Ca^{2+} signaling in the plasma membrane (PM) was developed, by adding a PM targeting sequence to a high signal-to-noise Ca^{2+} sensor protein GCaMP2[39].

In this probe, the C terminus of the CaM binding domain of myosin light chain kinase (M13), a skeletal muscle light-chain kinase, is connected to a circularly permuted EGFP (cpEGFP), which is fused to calmodulin (CaM)[40] (Fig. 6).

A conformational change when free Ca^{2+} binds to the CaM, allows a hinge region of this protein to bind M13, resulting in a Ca^{2+}-CaM-M13 interaction, which induces a following conformational change of cpEGFP, resulting in fluorescence intensity changes.

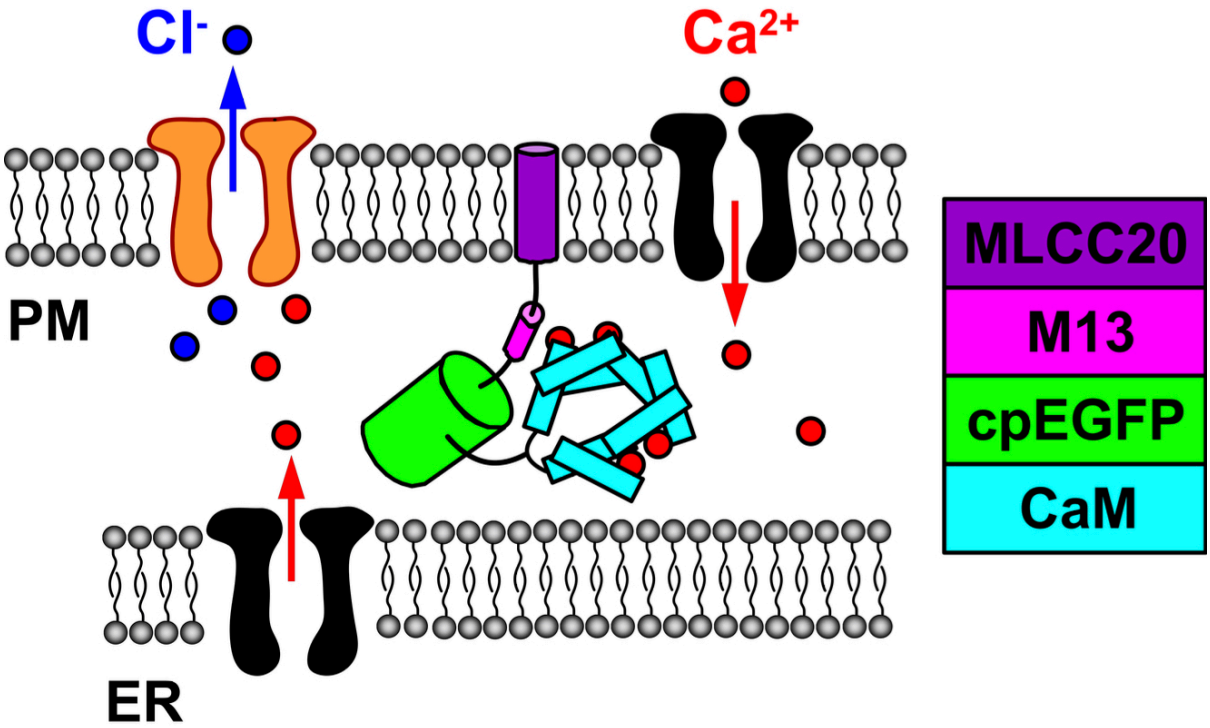

Figure 6. Schematic model of the EGFP-based Ca^{2+} probe: a PM targeting sequence (MLCC20), a fragment from myosin light chain kinase (M13), a circularly permutated EGFP (cpEGFP), and calmodulin (CaM), located N to C terminally.

This probe becomes localization-specific when the M13 fragment is fused in its N terminus to a plasma PM targeting sequence, the palmitoylation signal sequence of the first 20 amino acids of neuromodulin (MLCC20)[41] (Fig. 6).

2. Objectives

The aim of the present work was to study in a recombinant cell system and in a knockout animal model, whether proteins of the TMEM16 family change intracellular Ca^{2+} concentration ($[Ca^{2+}]_i$) and/or near the plasma membrane ($[Ca^{2+}]_P$).

In order to accomplished that, one of the objectives was to study, in HeLa cells, how overexpressed and endogenous ANOs change $[Ca^{2+}]_i$ and $[Ca^{2+}]_P$, using two different fluorescence indicators (Fura-2 AM and PM-GCaMP2, respectively). Anoctamin activity and cellular localization were further studied, in order to observe whether changes in $[Ca^{2+}]_P$ are dependent of those two parameters.

To corroborate the last results, it was intended to report whether ANO10 supports Ca^{2+} signaling in isolated intestinal Jejunum Crypts and renal Proximal Tubules.

ANO2 and ANO3 were not studied because they are mostly expressed in neurons and we were interested in the regulation on epithelial cells, where ANO1, -4, -5, -6, -7, -8, -9, and -10 were found to be expressed[26].

3. Materials and Methods

3.1 Cell Culture

Cell Culture was performed according to standard procedures using sterile equipment and solutions under laminar flow cabinet. Cells were grown in 75 cm^2 cell culture flasks, and maintained in an incubator with humidified atmosphere of 5% CO_2, at 37º C.

3.1.1 Mammalian Cell Lines

HeLa cells[42,43] were cultured in Dulbeco's modified Eagles medium (DMEM)-F12 (Life Technologies - Gibco®, Karlsruhe, Germany) supplemented with 10% Fetal Bovine Serum (FBS; Life Technologies - Gibco®, Karlsruhe, Germany) and 1% Penicillin-Streptomycin (PS; Life Technologies - Gibco®, Karlsruhe, Germany).

3.1.2 Transfections

All transfections were performed using Lipofectamine™3000 transfection reagent (Invitrogen, Germany) according to the manufacture's guidelines, in the absence of antibiotics.

For single cell fluorescence measurements of $[Ca^{2+}]_i$, HeLa cells were grown on glass cover slips, and were co-transfected with cDNA encoding either human ANO1, -4, -5, -6, -7, -8, -9 and -10, or empty pcDNA3.1 vector (mock) along with cDNA encoding CD8 co-receptor (the latter was transfected with a proportion of 1:4).

A novel fluorescent indicator for Ca^{2+} signaling in the plasma membrane (PM) was developed, by adding the PM targeting sequence of MLCC20 to a high signal-to-noise Ca^{2+} sensor protein GCaMP2[39]. For single cell fluorescence measurements of $[Ca^{2+}]_P$, HeLa cells were grown on glass cover slips, and were co-transfected with cDNA encoding either human ANO1, -4, -5, -6, -7, -8, -9 and -10, or empty pcDNA3.1 vector (mock) and MLCC20 GCaMP2 plasmid (the latter was transfected with a proportion of 1:5).

For functional analysis of endogenous anoctamins, expression of ANO6 and ANO10 was suppressed each by two independent sets of siRNA and PM-GCaMP2 plasmid

was transfected. siRNAs were transfected and cells were examined 24h for ANO6 and 48h for ANO10 after transfection by *Western Blot* (see section). Duplexes of 25 nucleotide of siRNA were designed and synthesized by Invitrogen (Paisley, UK) and Ambion (Darmstadt, Germany), for ANO6 and -10 respectively.

For immunocytochemistry, HeLa cells were grown on glass cover slips and transfected either with GFP/CFP tagged anoctamins: pcDNA3.1 ANO1, -7, -9 TC eGFP, pcDNA3.1 ANO4, -8, -10 GFP, pcDNA3.1 ANO6 TC GFP or pcDNA3.1 ANO5 CFP.

All cDNA experiments were executed after 48 to 72 hours (h) of transfection and siRNA experiments after 24 to 48h.

3.2 Molecular Biology

3.2.1 cDNA and siRNA

All the cDNA and siRNA used and mentioned in this study are described in Appendix I.

3.2.2 RT-PCR

Expression of mRNAs encoding all 10 human TMEM16-proteins were examined in HeLa cells by standard Reverse Transcription Polymerase Chain Reaction (RT-PCR) (Appendix II).

Total RNA was isolated from HeLa cells using NucleoSpin RNA II columns (Macherey-Nagel, Düren, Germany). Total RNA (1µg/ 50 µL reaction) was reverse-transcribed using random primer (Promega, Manheim, Germany) and M-MLV Reverse Transcriptase RNase H Minus (Promega, Mannheim, Germany). Each RT-PCR reaction contained sense and antisense primer for anoctamins (0,5 µM) or for GAPDH (0,5 µM) (see Appendix II, Table II.1), 0,5 µL cDNA and GoTaq Polymerase (Promega, Mannheim, Germany). RT-PCR program can be found in Appendix II, Table II.2. PCR products were visualized by loading on ethidium bromide-containing agarose gels and analysed using Meta Morph Vers. 6.2 (Molecular Devices, USA).

As a positive control a fraction of Glyceraldehyde 3-phosphate dehydrogenase (GAPDH) was used.

RT-PCR analysis was kindly provided by Prof. Dr. rer. nat. Rainer Schreiber.

3.2.3 Animal genotyping

Genotype of mice animal models were confirmed by Polymerase Chain Reaction (PCR).

Samples of mice tails were collected at the age of 5 weeks. DNA from the tails was extracted using 200 µM NaOH and incubated for 1h in 96ºC. Afterwards the tails were vortex in 20 µM 1M Tris, and spin down at 13 000xg for 6 min, in RT and kept in the fridge.

Briefly, the PCR for each sample was performed with 1µL of DNA, 1µL of each primer, 0,5 of each 10mM dNTP (Promega, USA), 0,1 µL of GoTaq® G2 DNA polymerase (Promega, USA) and 5µL 5X buffer (Promega, USA) in a final reaction volume of 12,5 µL of Nuclease-Free water (Promega, USA).

The PCR programs and corresponding primers are described in Appendix III.

3.3 Animal models

All experimental protocols were approved by the local councils for animal care and were conducted according to the German laws for animal care and the Guide for the Care and Use of Laboratory Animals, published by the National Institutes of Health.

3.3.1 Generation of tissue specific knockout models

The ANO10 knockout (KO) mice in the renal Proximal Tubule ($Pax8Cre^{+}/ANO10^{loxp/loxp}$) was generated through the natural mating of single transgenic mouse lines $ANO10^{loxp/loxp}$ and $Pax8Cre^{+}$, as seen in Figure 7.

To generate a ANO10 knockout in the intestine (Villin $Cre^{+}/ANO10^{loxp/loxp}$), VillinCre, resulted from a cross of Cre transgenic mice containing a Cre- expression cassette under the control of the epithelial-specific Villin promotor (Villin Cre^{+}), was crossed with $ANO10^{loxp/loxp}$ animals (like the strain mentioned above).

All individual generations were verified by Genotyping (Appendix III, Fig.III.1 and Fig.III.3).

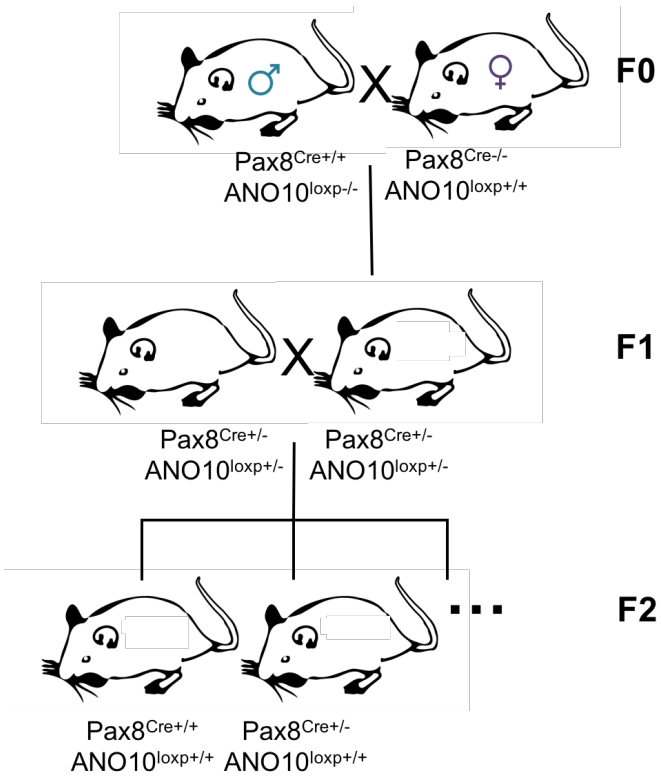

Figure 7. Breeding scheme used to produce specific Proximal Tubule ANO10 KO mice. (A) Homozygous Pax8Cre^{+} mice were breed with homozygous ANO10$^{loxp/loxp}$ to generate heterozygous control animals with the Cre and ANO10$^{loxp/loxp}$. Heterozygous Pax8Cre^{+}/ANO10$^{loxp/loxp}$ were breed together to generate homozygous Pax8Cre/ANO10$^{loxp/loxp}$ mice. F = Filial.

3.3.2 Jejunum Crypts Isolation

Mice were killed by cervical dislocation after being exposed to CO_2. The jejunum was removed (10 cm from the stomach) and flushed with Ca^{2+}- and Mg^{2+}-free NaCl Ringer's (mM: NaCl, 140; KCl, 1,5; Na_2HPO_4, 3; tris-(hydroxymethyl)aminoethane (Tris), 3,5; pH 7,4; dithiothreitol (DTT), 1; indomethacin (Indo), 0,001). After cleaned, the tissue was chopped into small pieces. These slices were incubated in 100% O_2 at room temperature (RT) in the same solution for 10 min. After incubation, the slices were rinsed twice in chelating medium (mM: NaCl, 96; KCl, 1,5; KH_2PO_4, 8; Na_2HPO_4, 5,6; Na_2EDTA, 27; sorbitol, 55; sucrose, 44; pH = 7,4 (equilibrated with NaOH); DTT, 1; Indo, 0,001) and then transferred to fresh chelating medium containing 1,2 mg of Collagenase I (Sigma, Taufkirchen, Germany) at 37°C and stirred for 6 min. The Collagenase I solution was discarded, the slices were re-suspended in chelating medium and vortexed vigorously for 1 min (2-3 times), allowed to settle and the crypt-enriched supernatant collected and re-suspended in DMEM containing DTT and Indo. Isolated crypts were kept on ice until required.

3.3.3 Kidney Perfusion

At the beginning of the surgical procedure, the test animal was subcutaneously anesthetized injecting 80-100µL of 5% (v/v NaCl) Ketamin (Henry Schein®,

Germany) and 2% Xylazin (Serumwerk Bernburg, Germany) solution. The abdominal cavity was opened by a medial line incision. The animal was eviscerated and the intestines were displaced out. The abdominal aorta, renal arteries, superior mesenteric artery and inferior vena cava were exempted from the surrounding connective tissue with the help of cotton sticks. Under the microscope, the left kidney was stitched with surgical suture equipment in the renal artery and vein (Fig. 8 A) in order not to be perfused and later on be used for primary culture. Usually the right kidney is the one perfused because the mesenteric artery arises from the aorta at the same level as the right renal artery and the catheter can be passed from one to the other without blood loss and without stopping the blood flow to the kidney. The aorta and vein were clamped above the point of separation of the renal artery (Fig. 8 B). A small cut was made in the aorta and a catheter (internal diameter, 0.3 mm) was inserted in direction retrograde to the blood flow with the help of a vasodilator (Fig. 8 C). After confirming that the catheter was well placed, it was clamped to the aorta (Fig. 8 D). The vein was cut (Fig. 8 E) to ensure venous drainage and the top clamp was taken out (Fig. 8 F). The mouse was perfused with 10mL of 2 µL/mL Heparin (v/v 0,9% NaCl; RotexMedica, Germany) solution followed by 40 mL of 4% (w/v in Phosphate Buffer Saline – PBS) Paraformaldehyde solution (mM: NaCl, 140; $K_2HPO_4.3H_2O$, 15; EGTA, 1; $MgCl_2.H_2O$, 2; Sucrose, 100; Paraformaldehyde (PFA), 4%). The perfusion procedure had a constant flow rate of 55 mL/min/g. The post-fixed kidney was kept in 1% (w/v in PBS) PFA with 16% sucrose, overnight (O/N).
The next day the kidney was frozen with Tissue-Tek® O.C.T.™ (Sakura) in nitrogen, and kept at -80ºC.

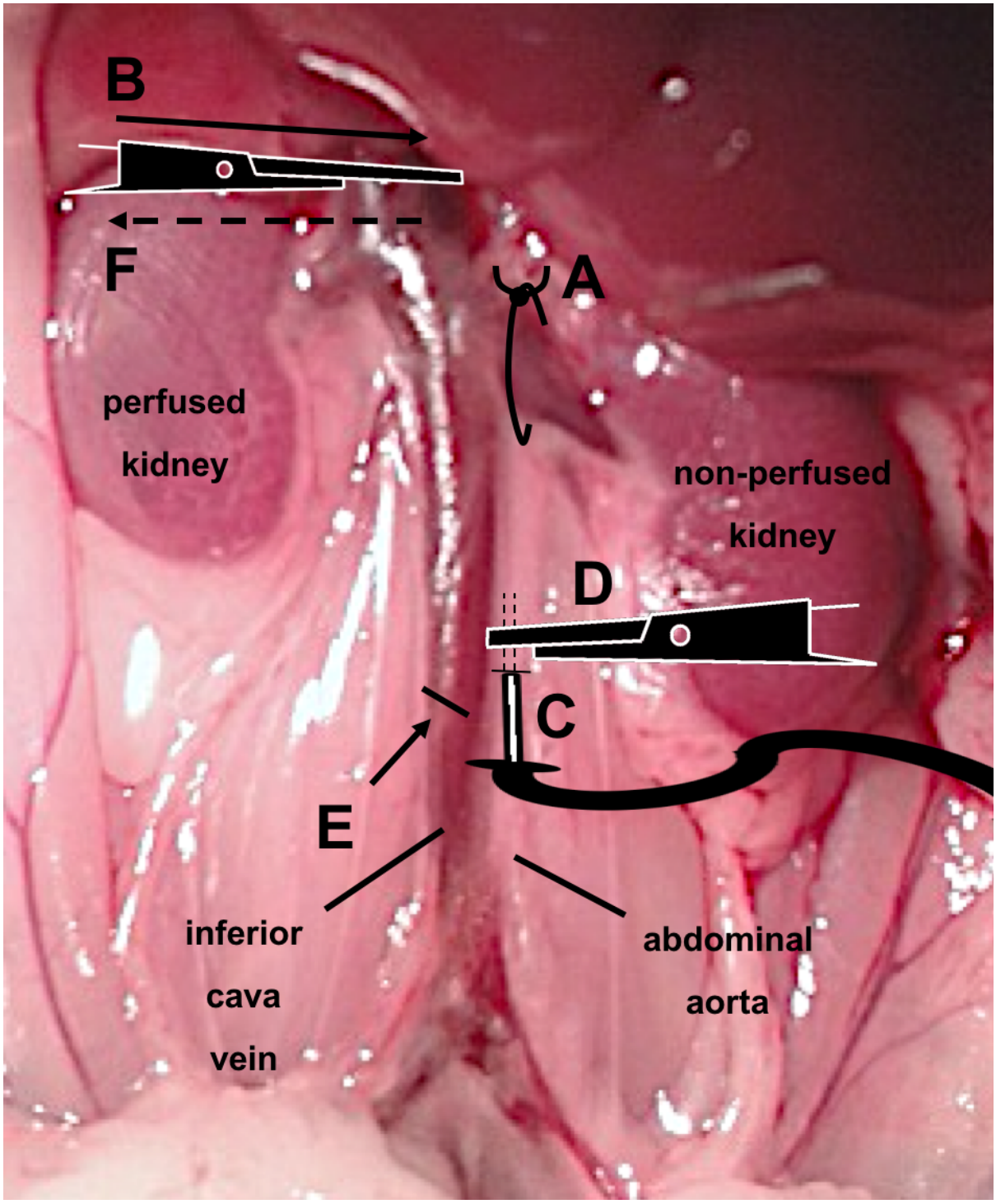

Figure 8. Schematic drawing of the kidney perfusion via the abdominal aorta. Perfusion was performed as follows: **(A)** the left kidney was stitched; **(B)** aorta and vein were ligated above the point of separation of the renal artery; **(C)** a small cut was made in the aorta and a catheter was inserted in direction retrograde to the blood flow; **(D)** the catheter was fixed with the aorta; **(E)** a hole was cut in the inferior cava vein to ensure venous drainage; **(F)** the first clamp was taken and the kidney was perfused with 10mL of 2 µL/mL Heparin (v/v 0,9% NaCl) followed by 40 mL of 4% (w/v) PFA solution, with a constant flow rate of 55 mL/min/g.

3.3.4 Proximal Tubules Isolation

The non-perfused kidney was removed and kept in ice cold DMEM F12 (PAN, PO4-41250) medium on a petri dish. The capsule from the kidney was removed by squeezing, under the flow, and put in another drop of medium. With a sharp blade, the cortex was cut off and chopped into smaller pieces, to facilitate the digestion in a small flask with 5 mL Hank's Balanced Salt Solution (HBSS) buffer (previously bubbled with 95% O_2 and 5% CO_2; 5 mL DMEM F12 (PAN, PO4-41250); 25 mg BSA; and 10 mg Collagenase type 2 (Worthington, S9H11286) when incubated for 20 min at 37ºC with a magnetic stir.

The digested tissue was passed through a sieve to a 50 mL falcon, pressed with the end of a syringe and washed out with ice cold PBS. After centrifuged for 4 min at 600xg at 4º C, the pellet was re-suspended and a Percoll gradient of 45% Percoll and 55% 2X PBS-Glucose was run at 17500rpm for 30 min, at 4º C. The gradient resulted in different bands, which the second one from the bottom was pipette out and collected in a 50 mL falcon tube. After washing with ice cold PBS three times (at 2200rpm, for 4 min), the pellet with isolated proximal tubules (PT) was re-suspended in media and kept on ice until use.

3.4 Functional Analysis – Calcium signaling measurements

3.4.1 Fura-2 AM measurements

Transfected HeLa cells (see section 3.1.2 Transfections) were loaded with 2 µM Fura-2 AM (Molecular Probes, Invitrogen, Germany) in ringer solution under experimental conditions with 0.2% Pluronic (Molecular Probes, Invitrogen, Germany) for 1h at RT and were incubated 1-2 min with Dynabeads CD8 (Invitrogen, Germany), before measuring, in order to recognise (permanently) the transfected cells. After loading, the cover slips were mounted in a cell chamber and perfused continuously with ringer solution (mM: NaCl 145, KH_2PO_4 0,4, K_2HPO_4 1,6, d-glucose 5, $MgCl_2$ 1, Ca-gluconate 1,3, pH 7,4) at a rate of 8 mL/min at 37ºC.

For $[Ca^{2+}]_i$ fluorescence measurements of intestinal jejunum crypts and renal proximal tubules isolated from mouse, the crypts and tubules were allowed to settle onto poly-L-lysine coated cover slips. Like single cell measurements, the crypts and tubules were mounted in a cell chamber and perfused continuously with ringer

solution at a rate of 8 mL/min at 37ºC. These cells were loaded with 2 µM Fura-2 AM in ringer solution under experimental conditions with 0.2% Pluronic for 1h at RT.

For functional analysis, fluorescence was measured continuously on an inverted microscope Axiovert S100 (Zeiss, Germany) with a Flua 40x/1.30 oil objective (Zeiss, Germany) and a high speed polychromator system (VisiChrome, Visitron Systems, Germany). Fura-2 was excited at 340/380 nm, and the emission was recorded between 470 and 550 nm using a CCD-camera (CoolSnap HQ, Visitron Systems, Germany). Control of experiment, imaging acquisition, and data analysis were done with the software package Meta-Fluor (Universal imaging, USA) and Origin (OriginLab Corporation, USA).

The flowing equation was used to calculate $[Ca^{2+}]_i$ from the 340/380 nm fluorescence ratio, after background substraction:

$$[Ca^{2+}]_i = K_d \left[\frac{(R - R_{min})}{(R_{max} - R)} \times \frac{Sf_2}{Sb_2}\right]$$

where *R* is the fluorescence ratio observed, R_{min} is the minimum fluorescence in the absence of Ca^{2+}, and R_{max} is the maximum fluorescence at saturating Ca^{2+} concentrations; Sf_2/Sb_2 is the ratio of fluorescence of free and Ca^{2+}-bound Fura-2 measured at 380 nm[44].

The R_{min}, R_{max}, and the constat Sf_2/Sb_2 were calculated using ringer solution with 2 µM Ionomycin (Calbiochem, Germany), 10 µM Monensin (Sigma, Taufkirchen, Germany) and 5 µM Nigericin and 5 mM Ethylene Glycol Tetraacetic Acid (EGTA) to equilibrate intracellular and extracellular Ca^{2+} in intact Fura-2-loaded cells. The dissociation constant for the Fura-2•Ca^{2+} complex was taken as 224 nM/L.

3.4.2 PM-GCaMP2 measurements

Transfected HeLa cells (see section 3.1.2 Transfections) were mounted and perfused like described above. PM-GCaMP2 was excited at 405/485 nm, and the emission was recorded between 535±25 nm using a CCD-camera (CoolSnap HQ, Visitron Systems, Germany). The fluorescence was measured continuously on an inverted microscope Axiovert S100 (Zeiss, Germany) with a Flua 40x/1.30 oil objective (Zeiss, Germany) and a high speed polychromator system (VisiChrome, Visitron Systems, Germany).

Control of experiment, imaging acquisition, and data analysis were done with the software package Meta-Fluor (Universal imaging, USA) and Origin (OriginLab Corporation, USA).
All the original traces were normalized to the baseline ratio.

3.5 Protein analysis

3.5.1 Immunocytochemistry on HeLa cells

Transfected HeLa cells (see section 3.1.2 Transfections) were washed once with cold PBS and cells were fixed for 10 minutes with 4% (w/v) PFA for at RT. Cells were rinsed three times with cold PBS to remove any leftover of the fixing solution and were incubated with 0,1% (v/v PBS) Triton X-100 for 10 minutes at RT. After a second rinse for three times with cold PBS, 1% (w/v PBS) bovine serum albumin (BSA) was add and left in incubation for 30 min at RT. The primary antibody goat anti-GFP (with a dilution factor (DF) 1:200; Rockland, Philadelphia) was incubated using PBS supplemented with 1% BSA for 1 h, at 4°C. For co-localization of ANOs with Ca^{2+} signaling proteins, primary antibody rabbit anti-IP_3R or mouse anti-SERCA 2 ATPase (DF 1:200; Abcam, UK) were added.
Cells were once again washed three times with cold PBS and incubated with the secondary antibody Alexa Fluor 488 conjugated Donkey Anti-Goat IgG (DF 1:500; Molecular Probes, Invitrogen, Germany) and 0,1 µg/mL (v/v PBS) Hoechst 33342 (DF 1:200; Aplichem, Darmstadt, Germany), for 1 h.
For subcellular localization, Alexa Fluor 647 Phalloidin (DF 1:100; Molecular Probes, Invitrogen, Germany) was also added and for co-localization analysis, Alexa Fluor 555 conjugated Donkey Anti-Rabbit IgG (DF 1:500) or Alexa Fluor 546 conjugated Donkey Anti-Mouse IgG (H+L) (DF 1:500; Molecular Probes, Invitrogen, Germany) were added. The cells were again rinsed three times with PBS and the cover slips were mounted with Fluorescence Mounting Medium (DAKO Cytomation, Hamburg, Germany).

3.5.2 Immunocytochemistry on Cryosections

Cryosections of 5 µm were washed with PBS and incubated in 0.1% (v/v PBS) Sodium Dodecyl Sulfate (SDS) for 5 min at RT, washed with PBS, and blocked with 5% (w/v PBS) BSA and 0.04% (v/v PBS) Triton X-100 for 10 min, at RT. Sections

were incubated with primary antibodies: rabbit anti-ANO10 (DF 1:100; Aviva Systems Biology, USA) for Intestinal Jejunum and Kidney, and rabbit anti-V-ATPase (DF 1:100; Aviva Systems Biology, USA) only for Kidney, in 0.5% (w/v PBS) BSA and 0.04% (v/v PBS) Triton X-100, O/N at 4°C. Sections were rinsed three times with PBS, and the secondary antibody Alexa Fluor 488 conjugated Donkey anti-rabbit IgG (IDF 1:300; Invitrogen, Germany) was added, and counterstained with Hoechst 33342 (DF 1:100). After incubation in the dark at RT for 1 h 30 min, sections were rinsed again with PBS and mounted with Fluorescence Mounting Medium.
Immunofluorescence was detected in a ApoTome Zeiss Axiovert 200M microscope (Zeiss, Göttingen, Germany) equipped with ApoTome and Axio-Vision (Zeiss, Jena, Germany).

3.5.3 Western Blot

Expression of ANO6 and ANO10 were downregulated in HeLa cells (see section 3.1.2 Transfections) and confirmed by *Western Blot*.
The protein was isolated from transfected HeLa cells in a lysis buffer (mM: Tris-HCl, 50; NaCl,150; Tris, 50; DTT, 100; NP-40, 1%; protease inhibitor cocktail, 1%) (Roche, Germany) and was separated on 8,5% SDS-PAGE Polyacrylamide gel. Separated proteins were transferred to a PVDF membrane (GE Healthcare Europe GmbH, Munich, Germany). The membrane was incubated with primary antibodies (DF 1:500 to 1:1000) O/N, at 4°C. Proteins were visualized using a suitable (HRP) conjugated secondary antibody (DF 1:10000) and ECL Detection Kit (GE Healthcare, Munich, Germany).
Knockout of ANO10 in intestinal Jejunum Crypts was confirmed by *Western blotting*. Lysates were prepared from isolated villi using lysis buffer (mM: Tris–HCl, 10; NaCl, 140; EDTA, 1; EGTA, 0,5; Triton-X-100, 1%; sodium deoxycholate, 0,1%; SDS, 0,1%) and 1% protease inhibitor cocktail (Roche, Germany). Proteins were separated on a 8.5% sodium dodecyl sulfate (SDS) polyacrylamide gel. The membrane was incubated with primary antibodies (DF 1:1000) O/N, at 4ºC. Proteins were visualized as mentioned before (Appendix III, Fig.III.2).
All protein bands were detected on a FujiFilm LAS-3000 (FujiFilm, Tokyo, Japan).
Western Blot analysis were kindly provided by Podchanart Wanitchakool.

3.6 Materials

All compounds used were of highest available grade of purity and were purchased from Sigma (Taufkirchen, Germany) or Merck (Darmstadt, Germany). Cell culture reagents were acquired from Invitrogen, Germany.

3.7 Statistical Analysis

For Statistical Analysis, student's t-test (for paired samples and unpaired samples), and analysis of variance (ANOVA) were used as appropriate. Values of $p < 0.05$ were accepted as significant.

4. Results

4.1 ATP-induced changes of $[Ca^{2+}]_i$ in ANOs expressing HeLa cells

For a critical evaluation of the role of calcium signaling as an intracellular messenger, it is required a quantitative measurement of cytosolic free Ca^{2+} concentrations $[Ca^{2+}]_i$, and a comparison between distinctive cell responses to different stimuli.

In order to measure possible effects of anoctamins on intracellular $[Ca^{2+}]$ signals, ANO1, -4, -5, -6, -7, -8, -9 and -10 were each co-expressed with cluster of differentiation 8 (CD8) co-receptor in HeLa cells. The CD8 co-receptor was expressed in order to recognise the transfected cells, when cells were incubated for 1-2 min with Dynabeads CD8.

$[Ca^{2+}]_i$ was measured using a global cytosolic Ca^{2+} sensor Fura-2 AM indicator[44] (Fig. 9 A), and three different concentrations of ATP – 1, 10 and 100 µM – were added to induce Ca^{2+} signaling (Fig. 9 B).

As a result, it was possible to observe in mock cells an ATP-dose-dependent Ca^{2+} signaling increase. Moreover, it was possible to distinguish a characteristic peak and a plateau, that are known to represent ATP-induced ER Ca^{2+} store release and Ca^{2+} influx, respectively (represented for mock, ANO4 and ANO5 overexpression in Fig. 9 B).

ANO1, ANO7 or ANO10 overexpression did not elicited any significant difference in Ca^{2+} store release and influx.

For the rest of the anoctamins, it was possible to distinguished two main groups, taking into account changes in the Ca^{2+} store release: due to ATP-purinergic stimulation, ANO5 and ANO6 overexpression increase the Ca^{2+} store release, whether ANO4 overexpression decrease the release (Fig. 9 C).

Through the observations of Ca^{2+} influx changes, ANOs can be also divided by two groups: the one that activate – like ANO5 overexpression; and inhibited – ANO4, 6, 8 and 9 overexpression (Fig. 9 D).

Additional original tracings of all anoctamins overexpression can be found on section Appendix IV.

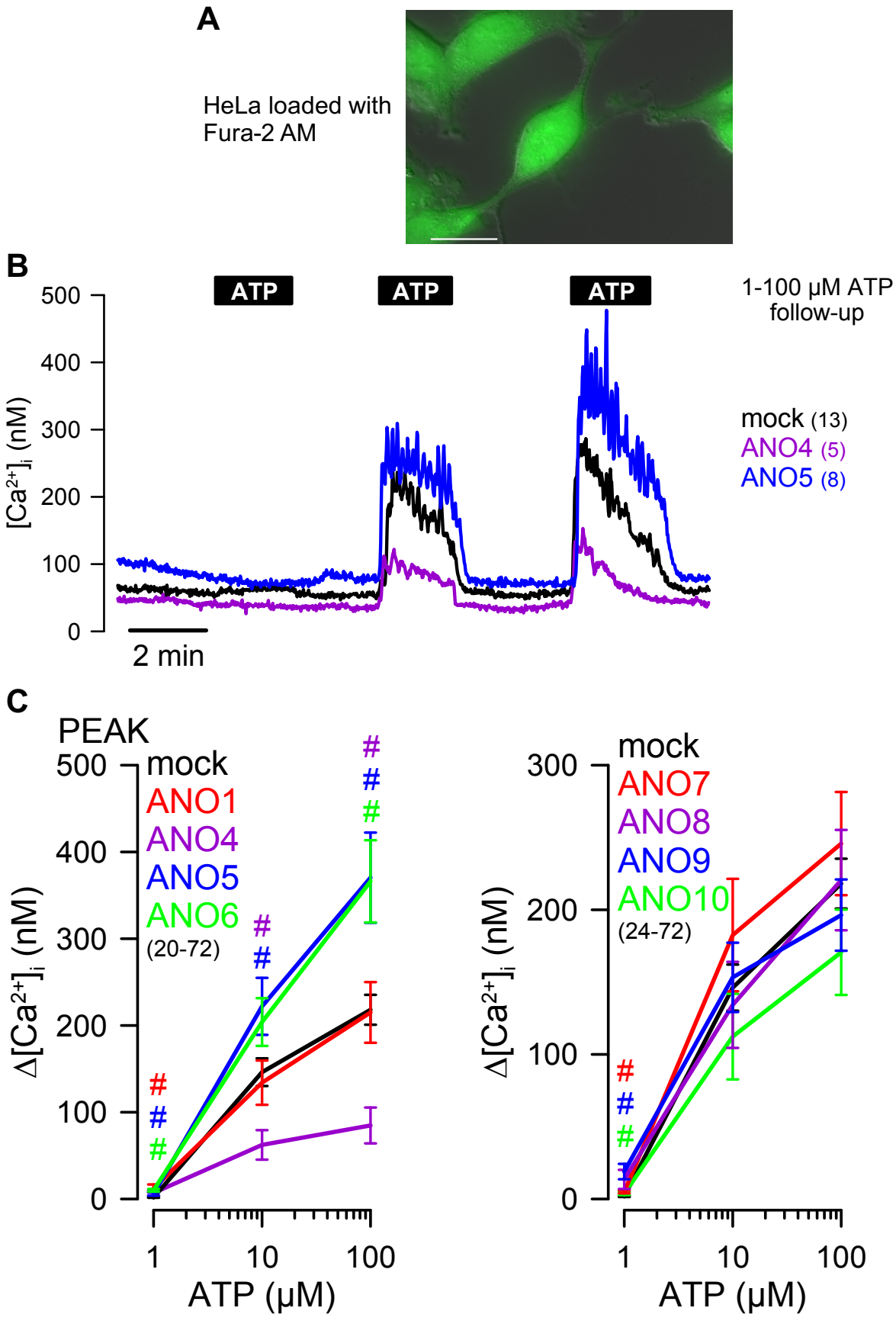
A
HeLa loaded with
Fura-2 AM
B
ATP
ATP
ATP
1-100 µM ATP
follow-up
mock (13)
ANO4 (5)
ANO5 (8)
[Ca2+]i (nM)
500
400
300
200
100
0
2 min
C
PEAK
mock
ANO1
ANO4
ANO5
ANO6
(20-72)
Δ[Ca2+]i (nM)
ATP (µM)
1
10
100
mock
ANO7
ANO8
ANO9
ANO10
(24-72)

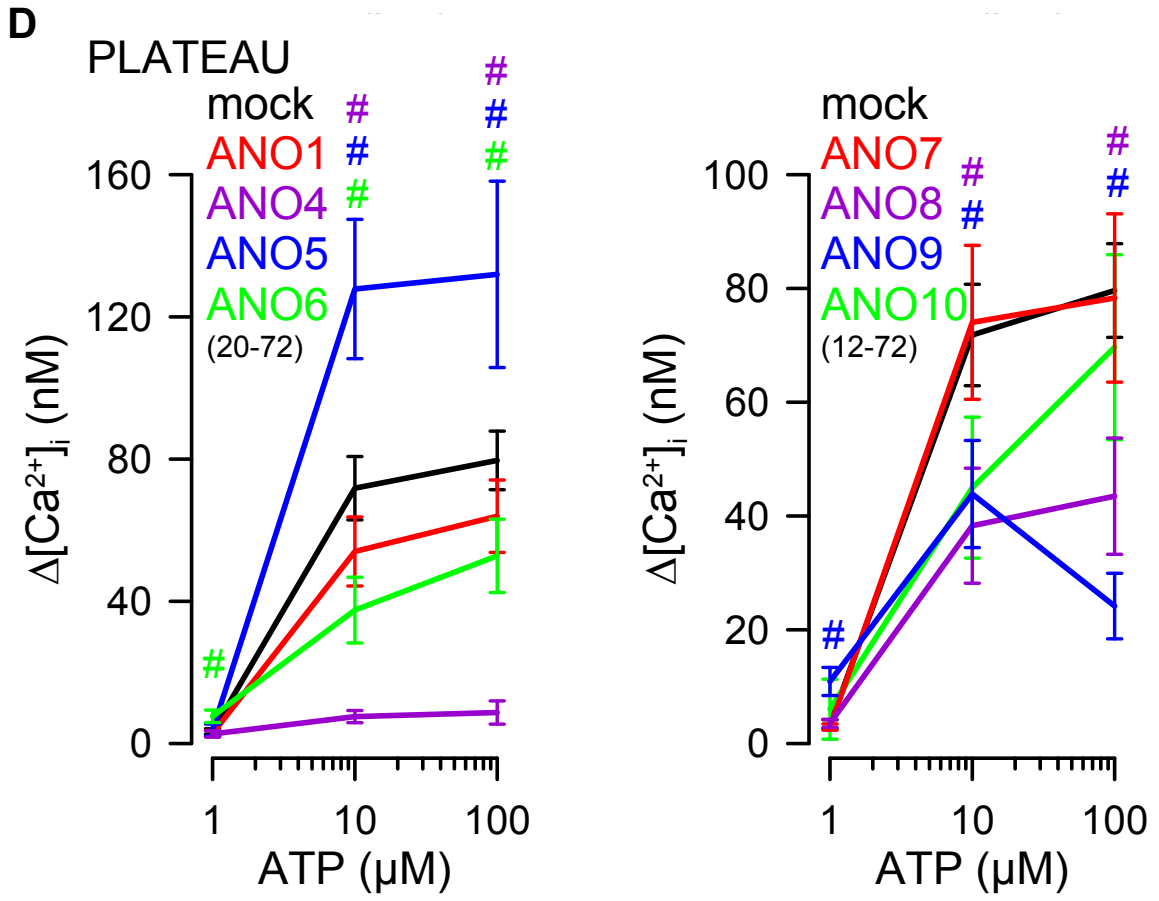

Figure 9. Effect of purinergic stimulation of ATP on Ca^{2+} signaling in TMEM16 overexpressing HeLa cells. (A) Confocal imaging of cytosolic Fura-2 AM probe in HeLa cells. Bar indicates 20 μm; **(B)** Original recordings of intracellular Ca^{2+} concentrations after purinergic ATP stimulation (10 and 100 μM ATP) of HeLa cells co-expressing whether mock, ANO4 or ANO5 with CD8 co-receptor; **(C)** Summary of Ca^{2+} store release (peak) changes showing significantly increase for overexpression of ANO5 and ANO6, and reduction for overexpression of ANO4; **(D)** Summary of Ca^{2+} influx (plateau) changes showing significantly increase for overexpression of ANO5, and reduction for overexpression of ANO4, -6, -8, and -9. Values are mean ± SEM (# unpaired t-test to mock, $p<0.05$); (n) = number of cells.

4.2 ATP-induced changes of $[Ca^{2+}]_P$ in ANOs expressing HeLa cells

A plasma membrane targeted calcium sensitive GFP protein (known as PM-GCaMP2) was co-expressed with the several anoctamins and variations of Ca^{2+} concentration specifically close to the plasma membrane ($[Ca^{2+}]_P$) were measured, compared when assessed by Fura-2 AM.

Trough confocal microscopy it was possible to confirm a considerable co-localization of GCaMP2 within the PM (Fig. 10 A).

Moreover, this sensor revealed only a transient Ca^{2+} peak after ATP stimulation and the removal of extracellular Ca^{2+} did not prevent ATP-induced Ca^{2+} signal. This

result indicated that ATP-induced changes of $[Ca^{2+}]_P$ is due to store release and not Ca^{2+} influx (Fig. 10 B).

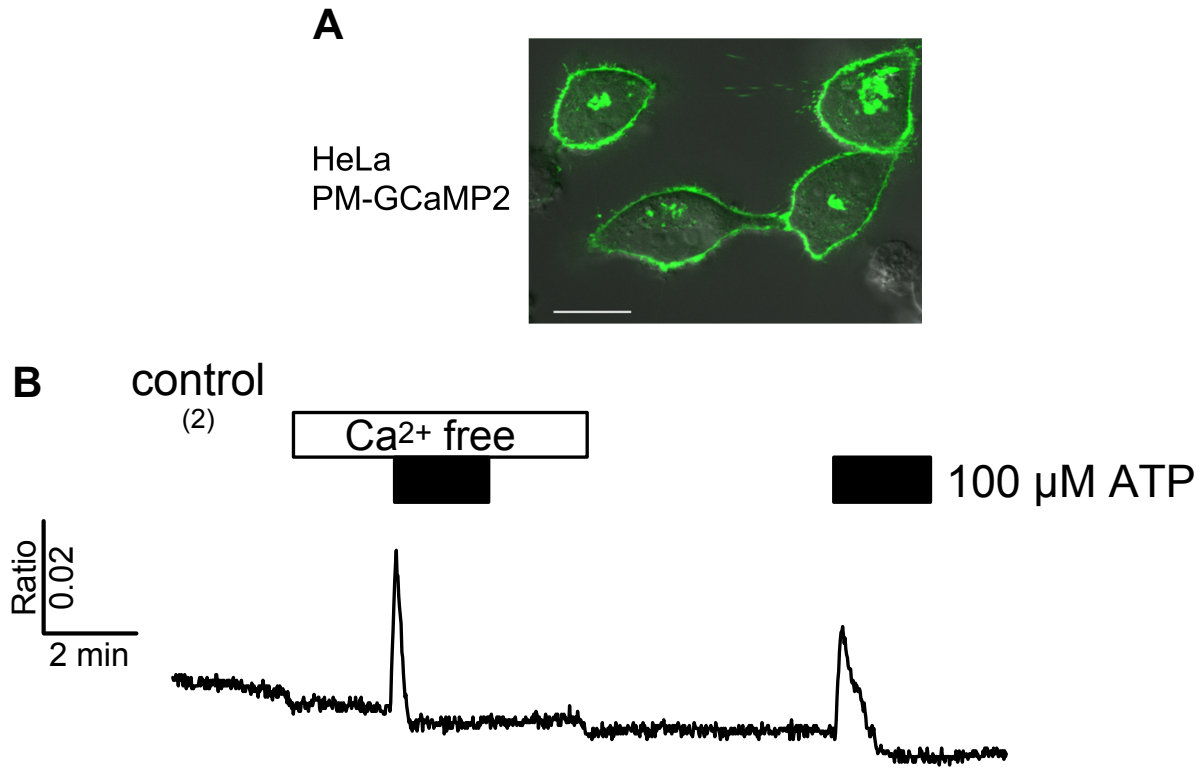

Figure 10. ATP induce a transient change of $[Ca^{2+}]_P$. (A) Confocal imaging of PM-GCaMP2 expression in HeLa cells plasma membrane. Bar indicates 20 µm; **(B)** Original mean tracing of purinergic ATP stimulation (100 µM ATP) from HeLa cells expressing PM-GCaMP2, with and without extracellular Ca^{2+} condition; (n) = number of cells.

HeLa cells were perfused with three different ATP concentrations. 1 µM, 10 µM and 100 µM that caused an ATP-dose-dependent transient increase of $[Ca^{2+}]_P$ in mock cells (Fig. 11 A and B; the original tracings of 1 µM ATP-induction can be found in Appendix V, Figure V.1).

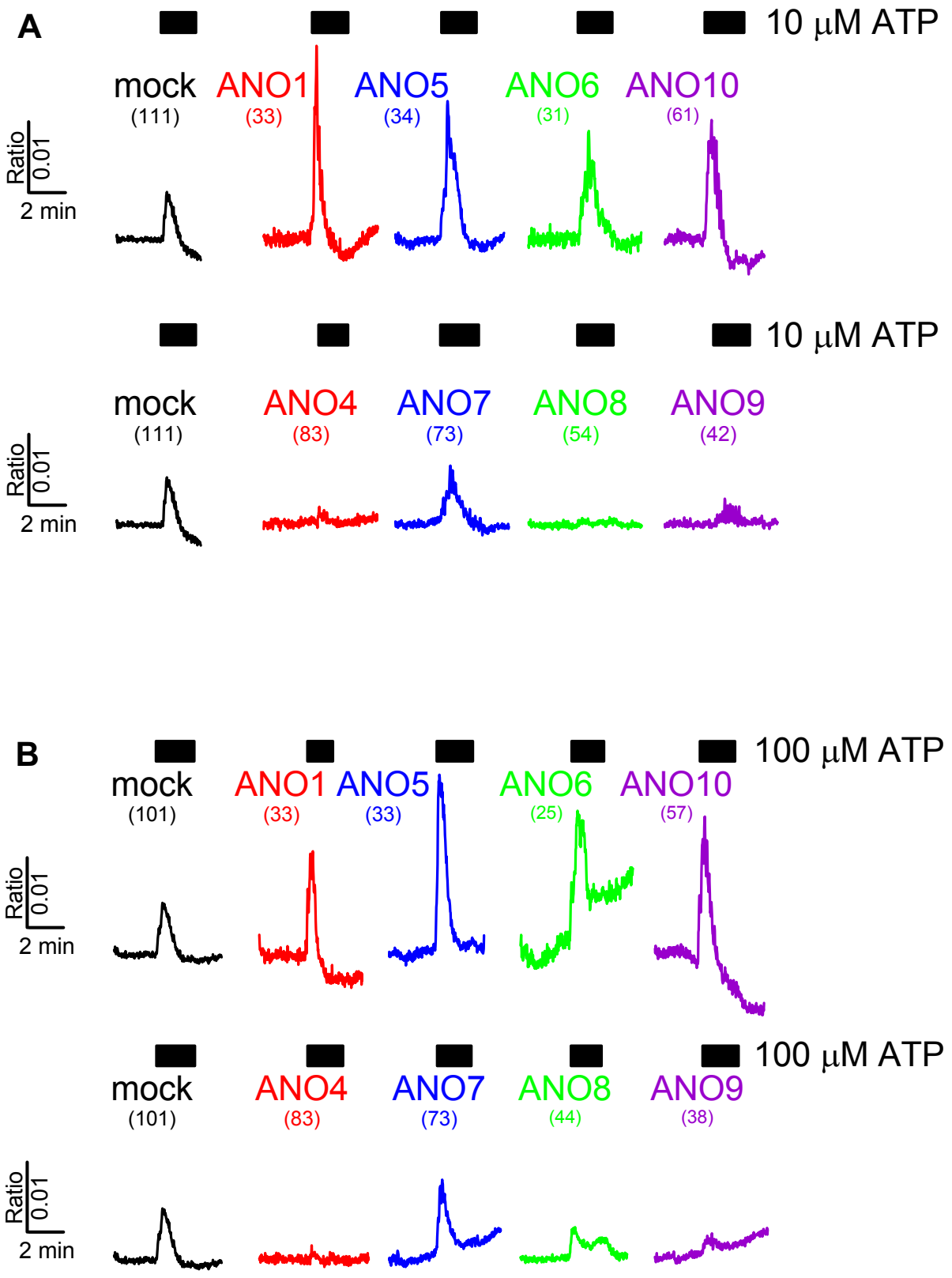
A
10 µM ATP
mock
(111)
ANO1
(33)
ANO5
(34)
ANO6
(31)
ANO10
(61)
Ratio
0.01
2 min
10 µM ATP
mock
(111)
ANO4
(83)
ANO7
(73)
ANO8
(54)
ANO9
(42)
Ratio
0.01
2 min
B
100 µM ATP
mock
(101)
ANO1
(33)
ANO5
(33)
ANO6
(25)
ANO10
(57)
Ratio
0.01
2 min
100 µM ATP
mock
(101)
ANO4
(83)
ANO7
(73)
ANO8
(44)
ANO9
(38)
Ratio
0.01
2 min

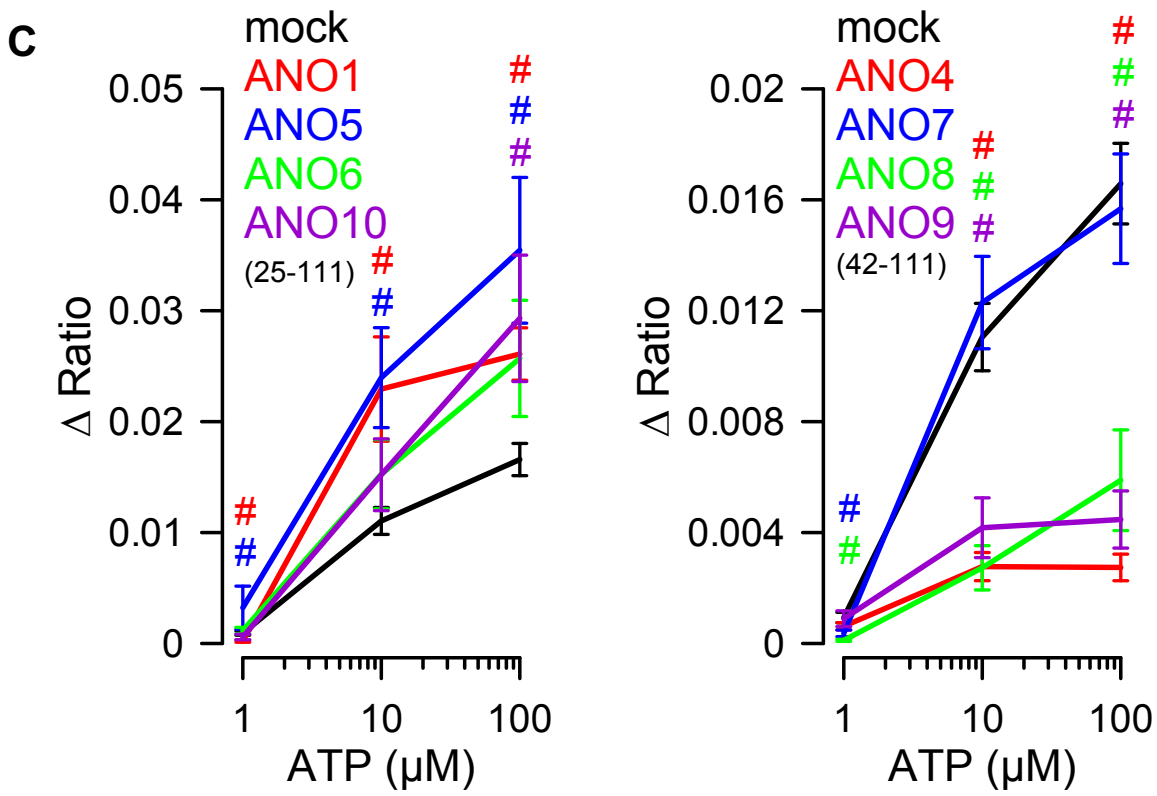

Figure 11. ATP-induced changes of $[Ca^{2+}]_P$ are modified by ANOs. (A) Original mean tracing of purinergic 10 μM ATP stimulation from HeLa cells co-expressing mock, ANO1, -4, -5, -6, -7, -8, -9, or -10 with PM-GCaMP2; **(B)** Original mean tracing of purinergic 100 μM ATP stimulation from HeLa cells co-expressing mock, ANO1, -4, -5, -6, -7, -8, -9, or -10 with PM-GCaMP2; **(C)** Summary presenting significantly increase of $[Ca^{2+}]_P$ by ATP for overexpression of ANO1, -5, and -10 and reduction for overexpression of ANO4, -8, and -9. Values are mean ± SEM (# unpaired t-test to mock; $p<0.05$); (n) = number of cells.

It is possible to observe that different anoctamins expression correlates with a different Ca^{2+} signaling regulation close to the plasma membrane. These results suggest that ANOs modulate changes in $[Ca^{2+}]_P$ and that this family of proteins can be divided in two different groups: ones that enhance (ANO1, -5, -6 or -10) and others that reduce (ANO4, -8, or -9) the Ca^{2+} signaling close to the PM (Fig. 11 C). Changes in $[Ca^{2+}]_P$ were not dependent of ANO6 and ANO7 overexpression.

4.3 ATP-induced changes of $[Ca^{2+}]_P$ are dependent on ANOs activity

In order to understand if ANOs activity is relevant for the regulation of intracellular Ca^{2+} signaling, HeLa cells overexpressing mock, ANO1, -4, -5 or -9 were measured in the presence of well known TMEM16 inhibitors – Niflumic Acid[45] and $CaCC_{inh}$-AO1[46]. Overexpression of ANO1, -4, -5, or -9 was selected since it was interesting to study at least two anoctamins with an enhanced Ca^{2+} signaling effect, and other two with a decreased effect.

HeLa cells were perfused for ~3 min with 20 µM Niflumic Acid (NFA) and then 10 µM ATP was added on top (Fig. 12 A).

The first observation was that the addition of NFA in any case, caused an drop of the fluorescence signal, suggesting a reduction of $[Ca^{2+}]_P$.

Basal $[Ca^{2+}]$ and ATP-induced Ca^{2+} signaling were reduced in HeLa cells overexpressing mock, ANO1, -4, -5 or -9 after incubation of 2 µM NFA (Fig. 12 A and B).

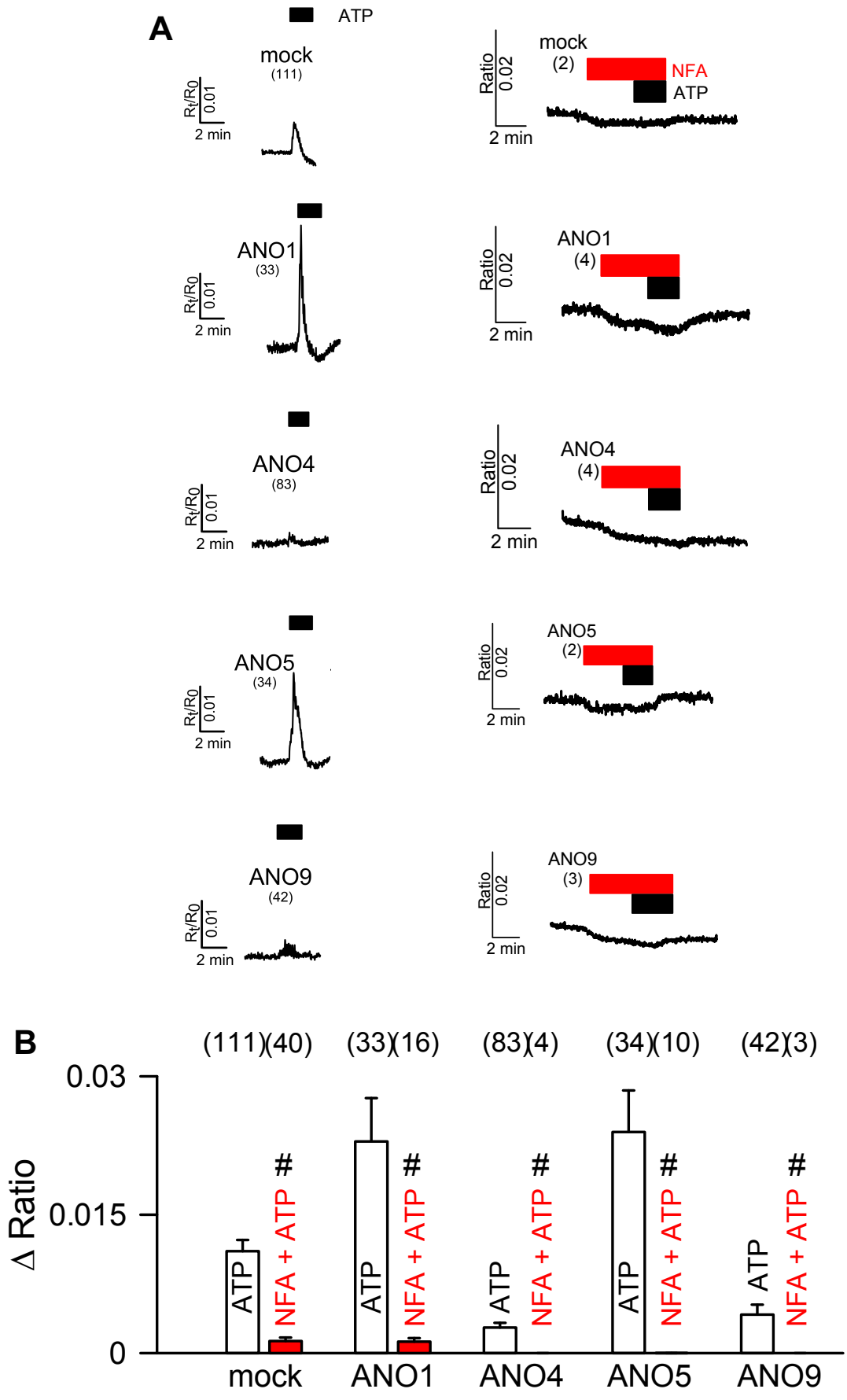

Figure 12. Inhibitory effect of NFA on Ca^{2+} signaling of ANO1, -4, -5, or -9 overexpressed in HeLa cells. (A) Original mean tracing of purinergic 10 µM ATP stimulation from HeLa cells co-

expressing whether ANO1, -4, -5, or -9, with GCaMP2 after 20 µM Niflumic Acid pre-incubation for 30 min; **(B)** Summary showing significantly decrease of ATP-induced Ca^{2+} signaling for overexpression of ANO1, -5, -4, and -9 after NFA incubation. Values are mean ± SEM (# unpaired t-test to 10 µM ATP signaling, $p<0.05$); (n) = number of cells.

As mentioned before, a second inhibitor was tested. Therefore, after mounted in the chamber, cells were perfused with 10 µM ATP with a short pre-incubation and in the presence of 10 µM $CaCC_{inh}$-AO1 (Fig. 13 A).

Similar effects observed with NFA incubation were observed in the presence of $CaCC_{inh}$-AO1, and the drop of the fluorescence signal was more pronounced with this inhibitor (Fig. 13 A and B).

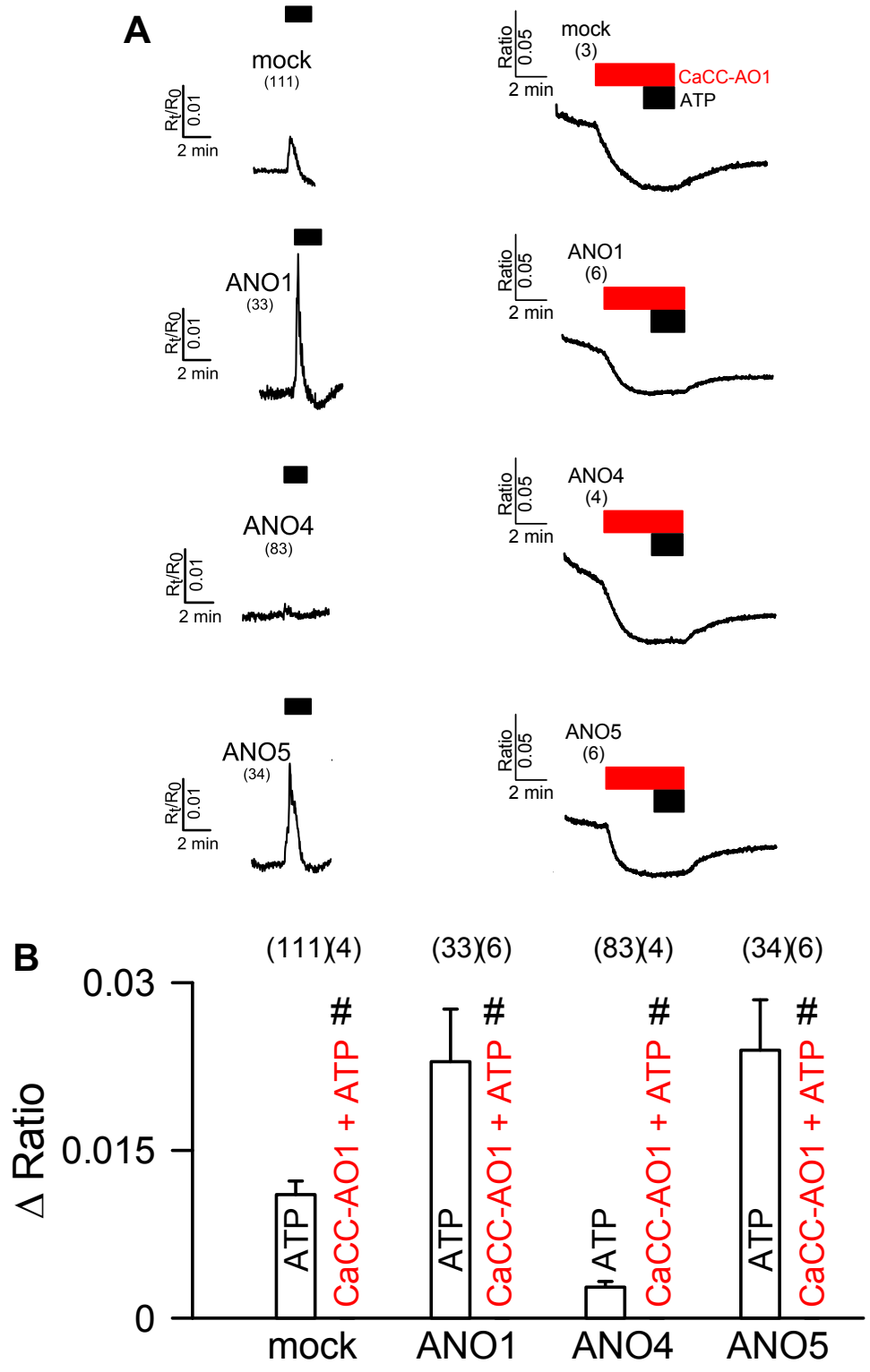

Figure 13. Inhibitory effect of $CaCC_{inh}$-AO1 on Ca^{2+} signaling of ANO1, -4, or -5 overexpressed in HeLa cells. (A) Mean tracing of purinergic 10 µM ATP stimulation from HeLa cells co-expressing whether ANO1, -4, or -5, with GCaMP2 in the presence of 10 µM $CaCC_{inh}$-AO1; **(B)** Summary displaying significantly decrease of ATP-induced Ca^{2+} signaling for overexpression of ANO1, -4, and -5 in the presence of $CaCC_{inh}$-AO1. Values are mean ± SEM (# unpaired t-test to 10µM ATP signaling without inhibitor, $p<0.05$); (n) = number of cells.

4.4 ATP-induced changes of $[Ca^{2+}]_P$ are modulated by endogenous expressed ANO6 and ANO10 in HeLa cells

HeLa cells express endogenous ANO4, -6, -8 and -10, shown by RT-PCR (Fig. 14 A). Being ANO6 and -10 the most expressed ones.

Therefore, the expression ANO6 and 10 was downregulated by treating the cells with siRNA. The reduced expression of ANO6 and ANO10 proteins was confirmed by *Western Blot* (Fig. 14 B).

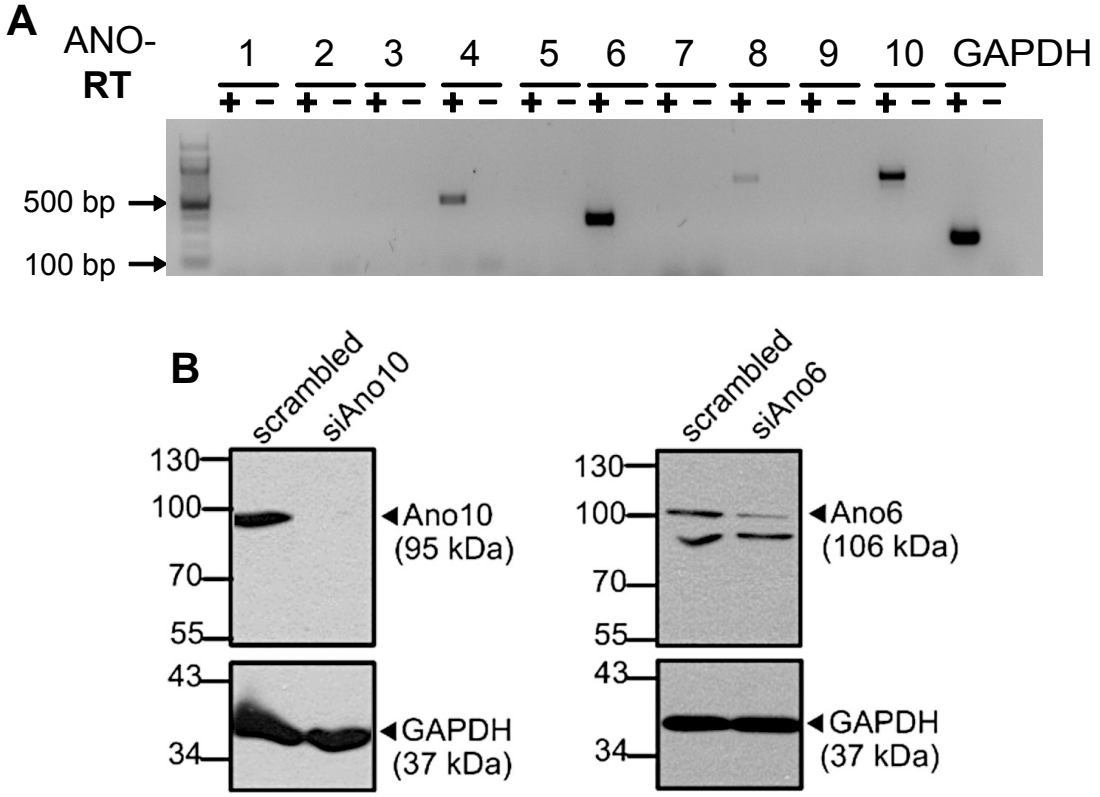

Figure 14. (A) RT-PCR analysis indicates expression of ANO4, -6, -8 and -10 in HeLa cells. 1-10 = ANO1-10; +/- = with/without reverse transcriptase (RT); **(B)** *Western Blot* analysis of ANO6 and -10 expression in HeLa cells, after 24h and 48h respectively, with and without siRNA transfection.

The same experimental procedure of overexpressed anoctamins in HeLa cells was implemented (Fig. 15 A; the original tracings of 1 µM ATP-induction can be found in Appendix V, Figure V.2). It was possible to observe a decrease in 10 µM and 100 µM ATP-induced $[Ca^{2+}]_P$, in the absence of ANO6 and ANO10 expression (Fig. 5B). These results suggested that endogenous expressed ANO10 and ANO6 are necessary for ATP induced changes of $[Ca^{2+}]_P$.

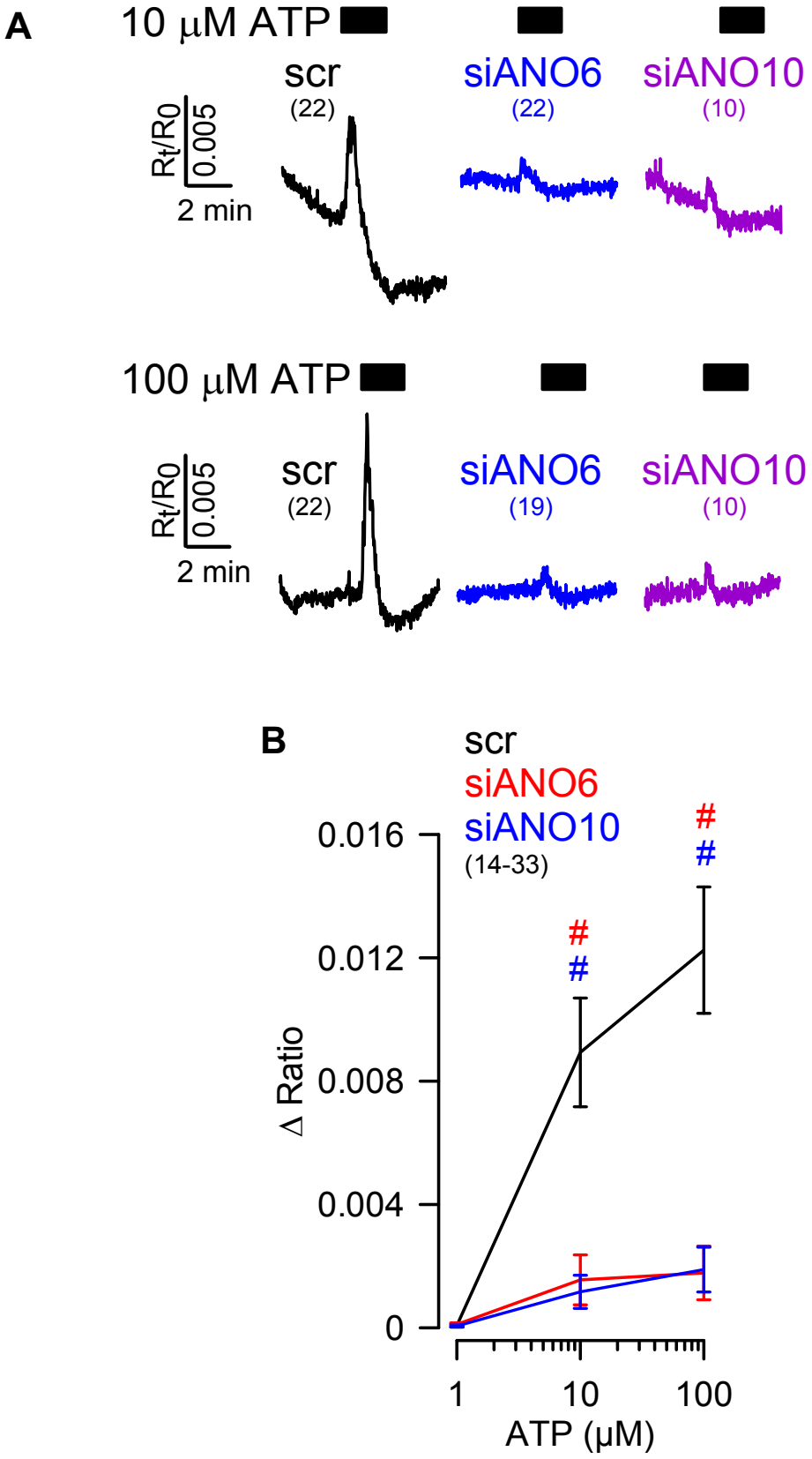

Figure 15. ATP-induced changes of $[Ca^{2+}]_P$ are modified by endogenous ANOs. (A) Tracing of purinergic ATP stimulation (10 and 100 µM ATP) from HeLa cells with PM-GCaMP2 and with whether ANO6 or -10 downregulated; **(B)** Summary showing significantly reduction of Ca^{2+} signaling resulted

from downregulation of ANO6 or -10. Values are mean ± SEM (# unpaired t-test to mock; $p<0.05$). (n) = number of cells.

4.5 Intracellular localization of overexpressed ANOs

We found two groups of anoctamins, in which one group facilitate and the other depressed ATP-induced changes of $[Ca^{2+}]_P$. One explanation could be different cellular localization of ANOs. Therefore, the cellular localization of C-terminal GFP tagged ANOs was further studied.

The C-termini of different ANOs were tagged with GFP and overexpressed in HeLa cells. Expression of GFP-tagged TMEM16 proteins (ANO1, -4, -5, -6, -7, -8, -9, -10) was verified by immunofluorescence (green) using a primary anti-GFP antibody and examined with an ApoTome Axiovert 200M fluorescent microscope (Zeiss, Germany) (Fig. 16). F-actin was visualized using the fluorescence-labeled Phalloidin (Invitrogen, Germany). As negative control, cells were transfected with empty pcDNA3.1.

Co-staining with sub-membranous F-actin indicated that most of ANO1 and 6 were localized in PM (yellow colour in the overlays), while, suggested that most of ANO4, 5, 7, 8, 9 and 10 were localized in intracellular membranes (Fig. 16).

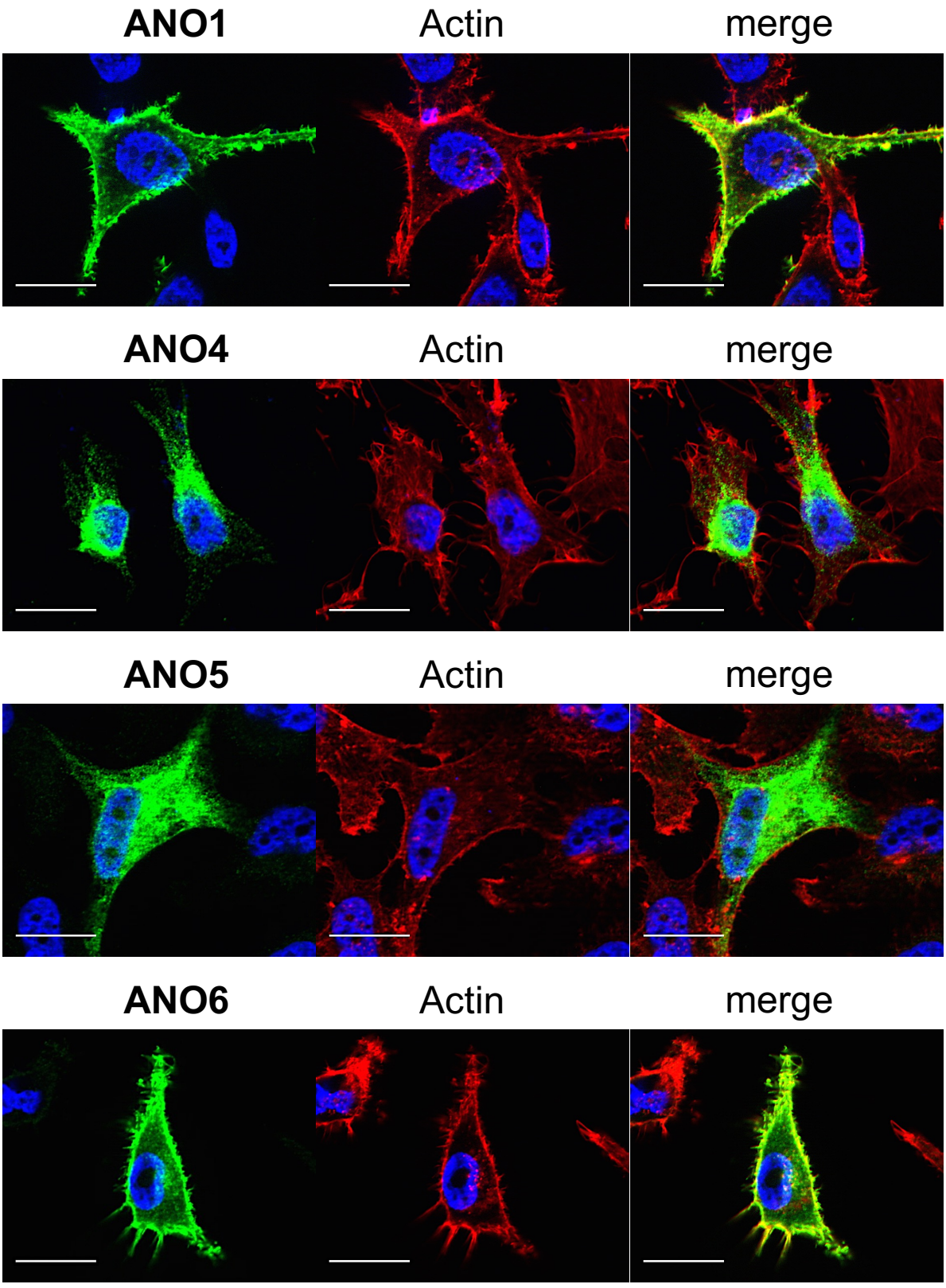
ANO1
Actin
merge
ANO4
Actin
merge
ANO5
Actin
merge
ANO6
Actin
merge

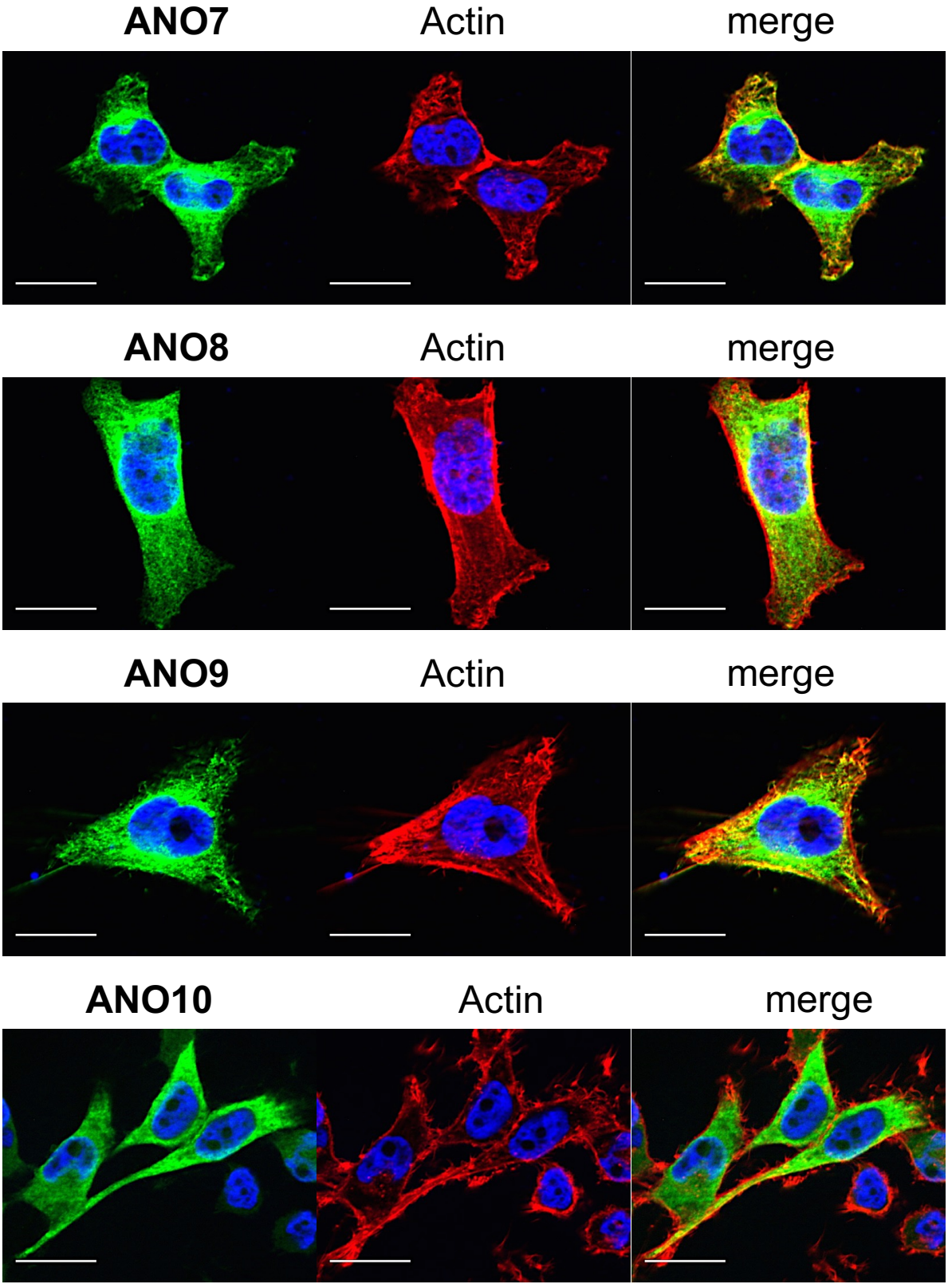

Figure 16. Subcellular localization of GFP-tagged ANOs in HeLa cells. GFP-tagged anoctamins (green) were overexpressed in HeLa cells and were detected with anti-GFP antibody. F-actin (red) was visualized using fluorescence-labeled Phalloidin. Plasma membrane staining of different anoctamins is shown by co-localization with F-actin (yellow colour in the overlay picture). Nuclei are shown in blue (DAPI staining). Bars indicate 20 µm.

4.6 Co-localization of ANO1 and ANO4 with IP_3 receptor and SERCA

Since the different subcellular localizations of overexpressed ANOs did not show a very clear distinction between increase and decrease of Ca^{2+} signaling, a study of co-localization of overexpressed ANO1 or ANO4 was performed and IP_3R and SERCA pump were selected, as different located Ca^{2+} signaling mechanisms[47]. ANO1 was chosen since its overexpression leads to an increased $[Ca^{2+}]_P$, and ANO4 to a decreased $[Ca^{2+}]_P$.

Once more, expression of these two GFP-tagged proteins (ANO1 and 4) was verified by immunofluorescence (green) using a primary anti-GFP antibody (Fig. 17) and examined with an ApoTome Axiovert 200M fluorescent microscope (Zeiss, Germany). IP_3R or SERCA pump (red) were visualized using a primary anti-IP_3R or anti-SERCA 2 ATPase antibody, respectively (Invitrogen, Germany). Negative control cells were transfected with pcDNA3.1 and incubated with primary antibodies anti-IP_3R or anti-SERCA 2 ATPase, and secondary antibodies.

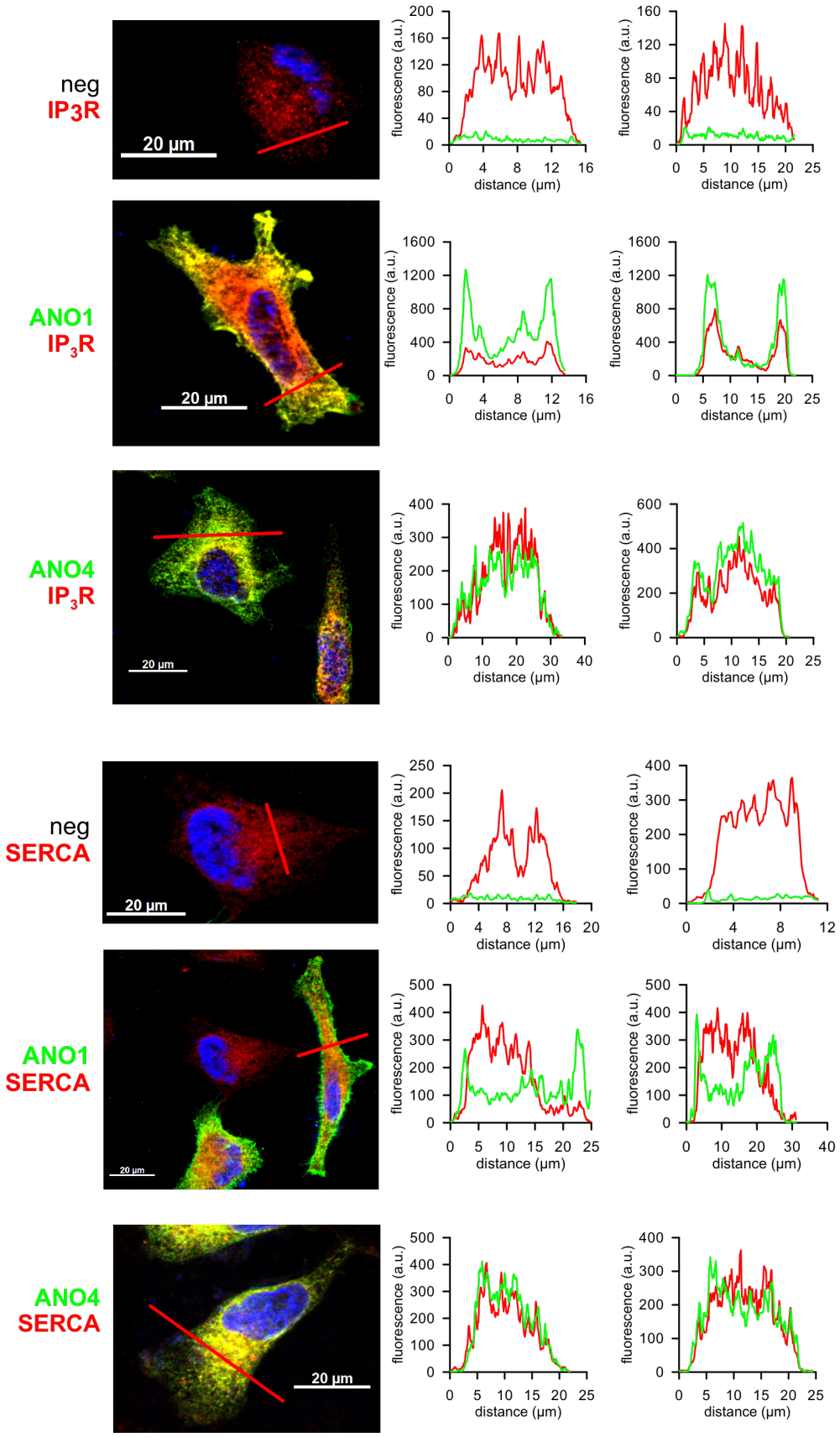

Figure 17. Subcellular co-localization of GFP-tagged ANOs and IP_3R or SERCA pump in HeLa cells. ANO1 and ANO4 GFP-tagged anoctamins (green) were overexpressed in HeLa cells and were detected with anti-GFP antibody. IP_3R and SERCA pump (in red, respectively indicated) were

visualized using respective primary antibodies. Co-localization ANO/protein is shown by yellow colour in the overlay picture and by fluorescence histograms. Nuclei are shown in blue (DAPI staining). Bars indicate 20 µm.

By the representative yellow colour of the overlays, IP_3R was found to co-localize with ANO1, whether SERCA pump was found to co-localize with ANO4 (Fig. 17).
Also, a fluorescence histogram was extracted from Axio-Vision software, where a fluorescence intensity was measured in a selected length of the cell. Fluorescence intensity peaks of IP_3R match with ANO1 peaks, while intensity peaks of SERCA matched with ANO4. These histograms present strong evidences of co-localization of ANO1 with IP_3R, and ANO4 with SERCA pump rather than with IP_3R.
Notice that, the selected length of the cell is represented in the X-axis of the histograms (Fig. 17). It is likely that IP_3R is distributed in different subcellular localization depending of the overexpressed ANO. In cells overexpressing ANO4, IP_3R localization seems similar to the negative control (without GFP-tagged ANOs). However, in cells overexpressing ANO1, IP_3R seems to be more distributed close to the PM.

4.7 ATP-induced Ca^{2+} signaling of overexpressed ANO1 and ANO4 with PM-GCaMP2 after disruption of lipid rafts by Filipin

Jin *et al.* found that ANO1 is expressed in membrane rafts, tethering the ER by the IP_3R[37]. This leads to the hypothesis that the different effect of ANOs on $[Ca^{2+}]_P$ could be explained by localization in different lipid rafts, which are responsible for different kinds of Ca^{2+} signalling.
Therefore, the next step was to understand whether the signaling increase or decrease observed were due to the presence of PM-GCaMP2 in this raft area. If this would be the case, the lower signaling derived from, e.g. ANO4 overexpression could be explain since this anoctamin is not expressed in these rafts.
Filipin is a polyene antibiotic cholesterol-binding reagent often used to investigate functional requirements for lipid rafts in receptor-mediated signal transduction[48]. This reagent binds selectively to cholesterol, forming complexes in the plasma membrane that sequester cholesterol and induce a structural disorder[48].

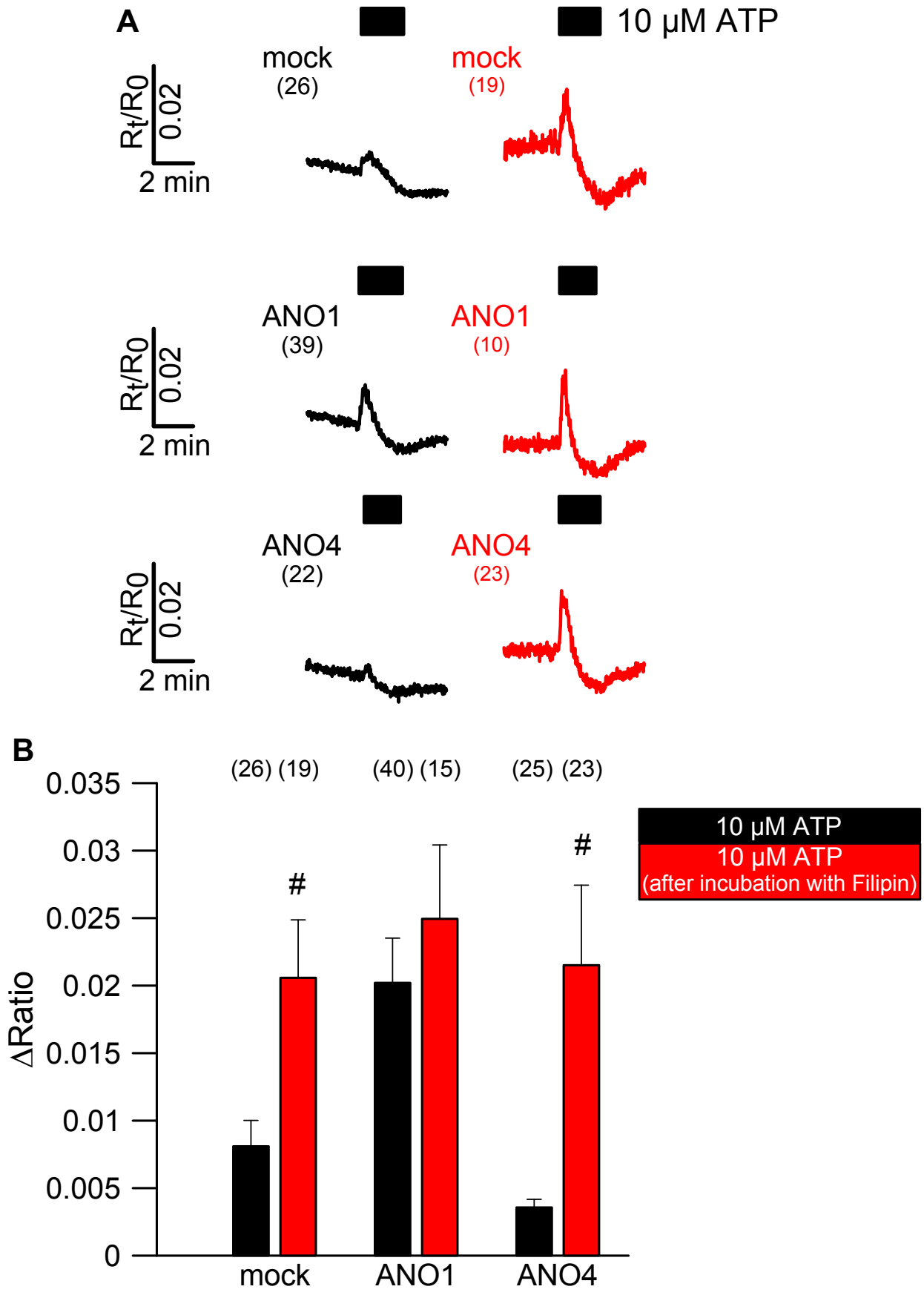

Figure 18. Effect of lipid raft disruption on Ca^{2+} signaling of mock, ANO1 or -4 overexpressed in HeLa cells with PM-GCaMP2 probe. (A) Tracing of the effect of lipid rafts disruption (red) in

$[Ca^{2+}]_P$ of co-expressing PM-GCaMP2 with whether mock, ANO1 or -4 in HeLa cell when induced by 10 µM ATP; **(B)** Summary showing significantly increase of Ca^{2+} signaling in mock and ANO4 overexpressing cells. Values are mean ± SEM (# unpaired t-test to 10 µM ATP signaling, $p<0.05$); (n)=number of cells.

In order to understand the functional requirement of membrane rafts, in the ATP-induced Ca^{2+} signaling observed, HeLa cells were transfected with mock, ANO1 or -4, treated with 2 µM Filipin for 30 min at RT and 10µM ATP induced changes of $[Ca^{2+}]_P$ were measured (Fig. 18 A).

Disruption of lipid rafts, had no effect on the ATP-induced changes of $[Ca^{2+}]_P$ in ANO1 overexpressing cells, but facilitated the signaling in mock and ANO4 expressing cells, compared with the presence of lipid rafts (Fig. 18 B).

4.8 ATP-induced Ca^{2+} signaling in Jejunum Crypts of wt and ANO10 tissue specific KO mice with Fura-2 AM

ANO10 was found expressed in intestinal jejunum of mice. Cryosections staining showed that ANO10 endogenous expression of wild-type (wt) animals in the jejunum is pronounced in the villi (Fig. 19 A), and that this protein is also expressed in the jejunum crypts (Fig. 19 B).

Villin Cre^{+}/$ANO10^{loxp/loxp}$ was shown to be a good animal model to study ANO10 either in the jejunum villi and crypts, since it is possible to observe a clear tissue specific knockout of this protein in the intestinal jejunum by immunohistochemistry (Fig. 19) and by *Western Blot* (see Appendix III, Figure III.2).

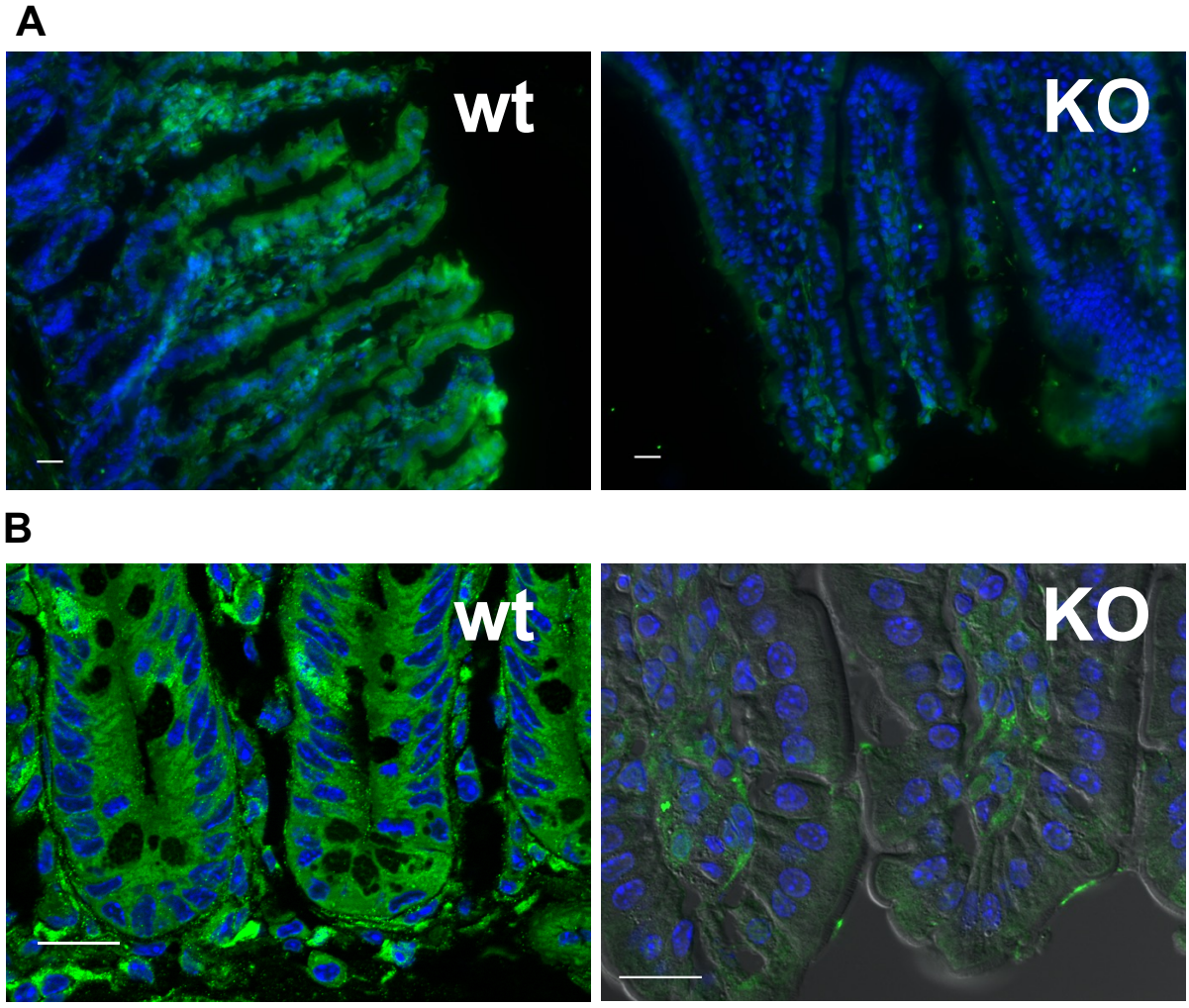

Figure 19. Subcellular localization of ANO10 in intestinal Jejunum villi and crypts of wt and ANO10-/- mice. wt and KO jejunum observed using **(A)** objective of x20, where it is possible to observe the crypts and villi; and **(B)** objective of x63 ApopTome, where it is possible to observe the crypts. ANO10 (green) was detected with rabbit anti-ANO10 antibody. Nuclei are shown in blue (DAPI staining). Bars indicate 20 µm.

The last goal was to evaluate the effect of endogenous anoctamins *in vivo*. To achieve this, intestinal Jejunum Crypts from wild-type (wt) and ANO10 knockout (ANO10-/-) mice were isolated, settled onto poly-L-lysine coated coverslips and incubated with Fura-2 AM for 1 h, at RT.

The purpose of this functional analysis was to observe whether ANO10 affects ATP and Carbachol (CCH)-induced intracellular Ca^{2+} signals. These two agonists have different mechanisms of Ca^{2+} signaling. CCH induces basolateral intracellular Ca^{2+} signaling trough muscarinic receptors[32], whereas ATP induces apical intracellular Ca^{2+} signaling trough purinergic receptors. Therefore, crypts were perfused with 100 µM Carbachol and 100 µM ATP (Fig. 20 A).

ATP-induced Ca^{2+} peak and plateau were significantly reduced in Jejunum Crypts lacking ANO10 expression compared with wt (Fig. 20 B). While CCH stimulation did not lead to any significantly difference in Ca^{2+} store release and influx.

Also notice the significant decrease of basal $[Ca^{2+}]_i$ in ANO10-/- mice (Fig. 20 C).

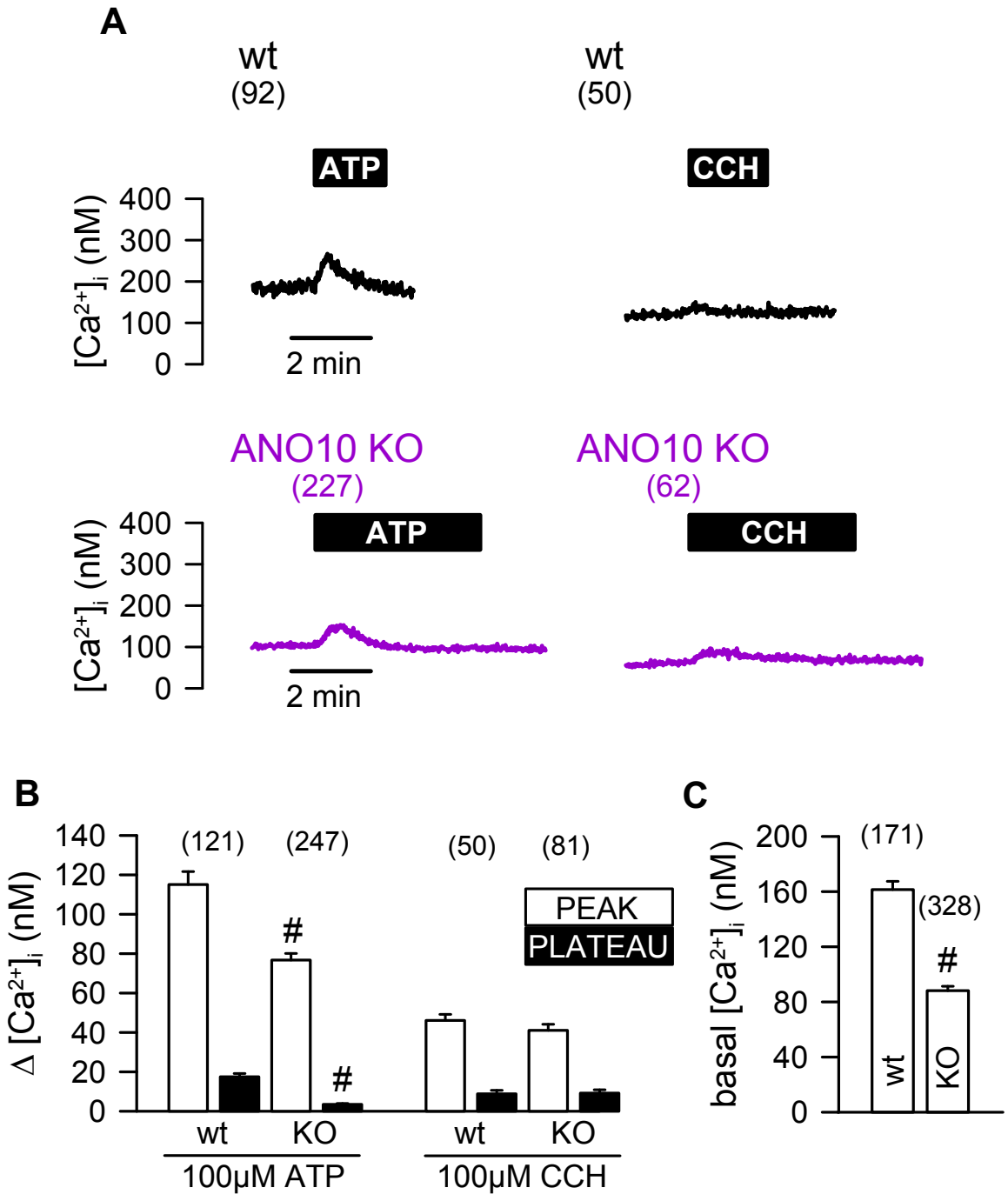

Figure 20. CCH and ATP-induced effect in intestinal Jejunum Crypts from wt and ANO10-/- mice. (A) Original mean tracing of purinergic 100 µM ATP or 100 µM Carbachol stimulation in Jejunum Crypts from wt and ANO10-/- animals, using Fura-2 AM dye; **(B)** Summary showing attenuated ATP-induced Ca^{2+} signaling in Jejunum Crypts of mice lacking ANO10. Data corresponding to seven Jejunum Crypts from two wt and to eight Jejunum Crypts from two ANO10-/- mice. Values are mean ± SEM (# unpaired t-test to wt, $p<0.05$); (n) = number of cells.

Mice genotyping and confirmation *Western Blot* can be found in Appendix III.

4.9 ATP-induced Ca^{2+} signaling in Proximal Tubules of wt and ANO10 kidney specific KO mice with Fura-2 AM

Although Jejunum Crypts data suggest the concept that ANO10 supports intracellular Ca^{2+} increase, renal Proximal Tubules were used as another system to corroborate these results.

ANO10 was visualized using rabbit anti-ANO10 antibody and PT were visualized trough a proximal tubular epithelial marker, V-ATPase, using rabbit anti-V-ATPase. Since both antibodies used were produced in rabbit, the staining was performed in different cryosections.

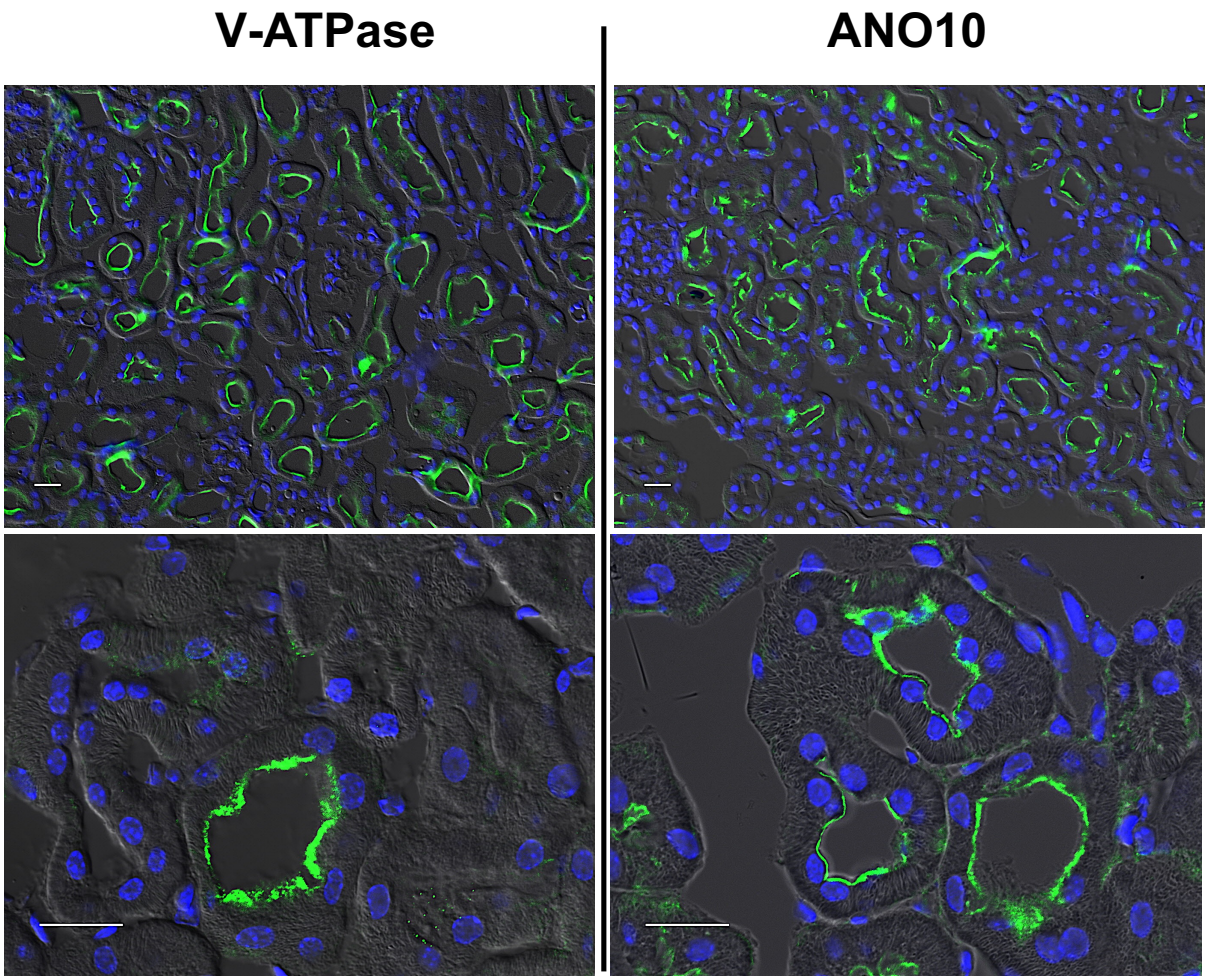

Figure 21. Subcellular localization of ANO10 in the apical side of Proximal Tubules. PT (left green) were visualized using rabbit anti-V-ATPase antibody and ANO10 (right green) was detected with rabbit anti-ANO10 antibody. In the first row the pictures were taken with an objective of x20, and in the second one with an objective of x63 ApopTome Nuclei are shown in blue (DAPI staining). Bars indicate 20 µm.

The expression of ANO10 in mouse kidneys, was found only on the apical side of proximal tubular epithelial cells in wt mice (Fig. 21). PT tubules were loaded like Jejunum Crypts and perfused with 100 µM ATP (Fig. 22 A). Functional analysis data of isolated PT were correlated with intestinal Jejunum Crypts, where ATP-induced Ca^{2+} store release and influx were attenuated in PT from mice lacking ANO10 expression (Fig. 22 B). Once again, it is possible to observe a decrease in basal $[Ca^{2+}]_i$ in ANO10-/- mice (Fig. 22 C).

Mice genotyping can be found in Appendix III.

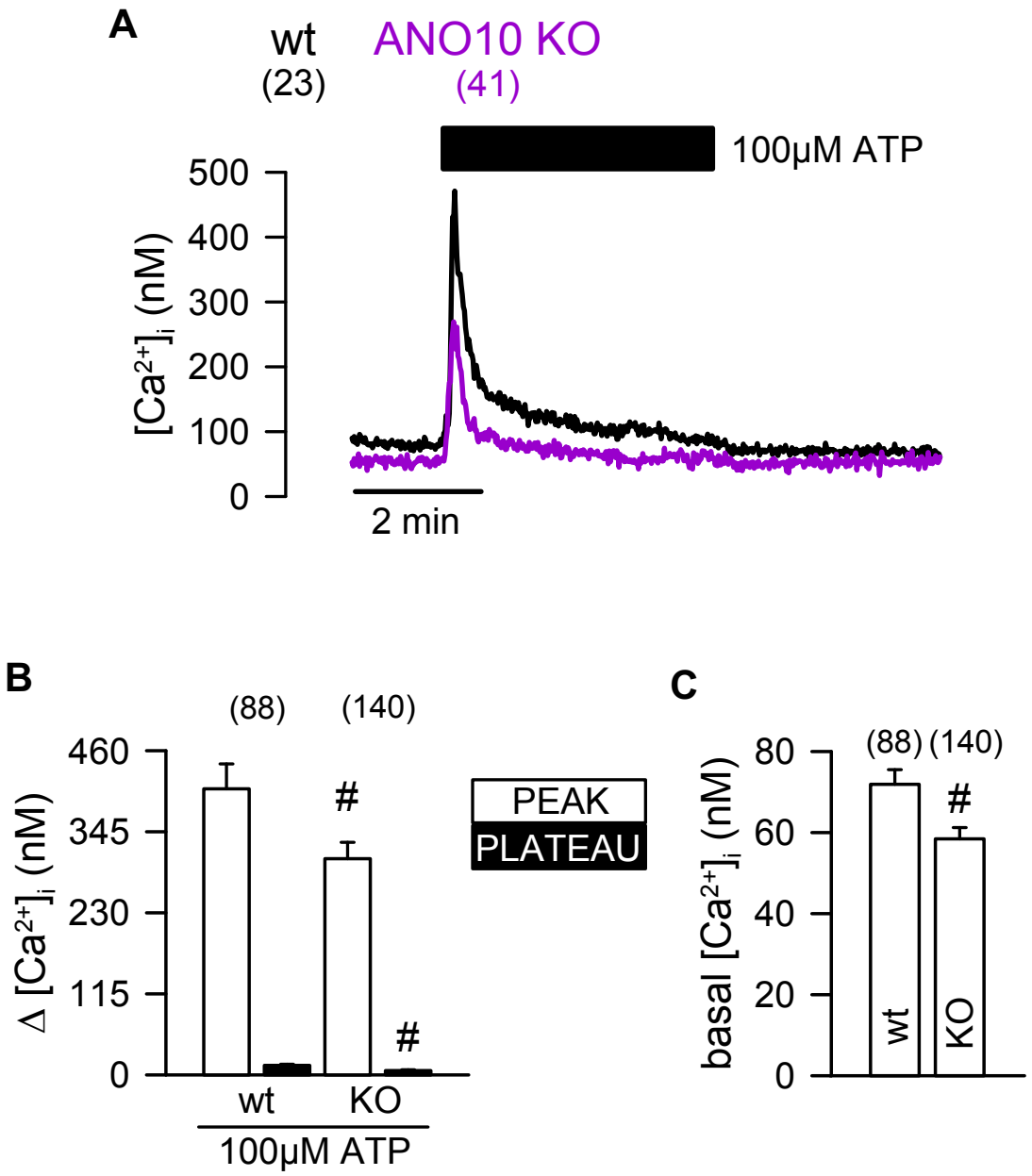

Figure 22. ATP-induced effect in renal Proximal Tubules from wt and ANO10-/- mice. (A) Original mean tracing of purinergic 100 µM ATP stimulation in PT from wt and ANO10-/- animals, using Fura-2 AM dye; **(B)** Summary showing attenuated ATP-induced Ca^{2+} signaling in mice lacking

ANO10. Data corresponding to two Proximal Tubules from each two wt and two ANO10-/- mice. Values are mean ± SEM (# unpaired t-test to wt, $p<0.05$). (n) = number of cells.

5. Discussion

This work tracks the evidence in the literature about the calcium-activated chloride channels ANO1 and ANO6, that support Ca^{2+} signaling in intestinal crypts[32] and in osteoblasts[34], respectively, and the ANO1 compartmentalized regulation of Ca^{2+} signaling[37].

The main goal of this thesis was to understand how different anoctamins change/regulate Ca^{2+} signaling *in vitro* and *in vivo* systems.

5.1 GCaMP2 fluorescence measurements are a better tool to measure localized signals than Fura-2 AM measurements

There were already efforts made to study the impact of anoctamins on local Ca^{2+} signaling, studying the global, cytosolic Ca^{2+} levels by Fura-2 AM probe[49]. However, anoctamins related protein IST2 is a tethering protein, organizing arrangements between cortical ER with the PM[35] and other studies suggested expression of ANO1 in lipid rafts[37], therefore, measurements of the local Ca^{2+} concentration close to the plasma membrane ($[Ca^{2+}]_P$) are more relevant to investigate the function of ANOs on Ca^{2+} signaling.

Fura-2 AM has a dissociation constant (Kd) of around 140 nM[44]. Therefore, high Ca^{2+} concentrations close to the PM are not resolved. A simple explanation could be that changes of intracellular calcium concentrations ($[Ca^{2+}]_i$) measured by Fura-2 with a nanomolar (nM) range, mask changes of $[Ca^{2+}]_P$. Therefore the novel plasma membrane targeted calcium sensitive GFP protein (PM-GCaMP2), which allows measurements close to the PM, could be the right tool to track changes of $[Ca^{2+}]_P$.

5.2 Regulation of $[Ca^{2+}]_i$ and $[Ca^{2+}]_P$ by ANOs

Anoctamins regulate Ca^{2+} signaling in a different fashion.

When intracellular calcium concentrations ($[Ca^{2+}]_i$) were measured, it was possible to discriminate ATP-induced Ca^{2+} changes related to Ca^{2+} store release (represented as a peak) and Ca^{2+} influx (represented as a plateau). ANO5 and ANO6 overexpression presented an increase of Ca^{2+} store release, and ANO4 a decreased

release. Also, ANO4, -6, -8 and -9 overexpression lead to a decreased Ca^{2+} influx, whereas ANO5 overexpression lead to an increase of influx. Therefore, it is possible to consider two distinct groups according to the calcium signaling: ANO5 and -6 facilitate Ca^{2+} store release and ANO4 does the opposite. Taking into account Ca^{2+} influx, ANO5 activates and ANO4, -6, -8, and -9 inhibit this influx.

Using a plasma membrane targeted calcium sensitive GFP protein (PM-GCaMP2) it was possible to measure changes on ATP-induced Ca^{2+} concentrations close to the PM ($[Ca^{2+}]_P$). In this case, a transient Ca^{2+} peak was obtained, corresponding to Ca^{2+} store release. ANO1, -5, and -10 overexpression showed an increased peak, whether ANO4, -8 and -9 overexpression showed a decreased peak. Consequently, it is possible to distinguish two different groups: anoctamins that facilitate Ca^{2+} store release close to the PM – ANO1, -5, and -10; and anoctamins that diminished – ANO4, -8 and -9.

It was shown that all members of ANOs have a function as an Ca^{2+}-activated Cl^- channels[49]. In order to test if the Cl^- fluxes due by the ANOs are necessary to regulate changes in $[Ca^{2+}]_P$ specific ANO inhibitors were used. It was shown that the activity of, at least, ANO1, -4, -5 and -9 is relevant for this regulation, since the lack of overexpressed ANOs activity leads to a lost of ATP-induced Ca^{2+} signaling. Also, the basal $[Ca^{2+}]_P$ was affected, since a drop of the fluorescence signal is observed with both inhibitors. This effect may indicate that ANOs activity also regulates the basal $[Ca^{2+}]$. But it can not be excluded that these inhibitors themselves quenched the PM-GCaMP2 fluorescence signal.

Different co-localization of ANOs with Ca^{2+} signaling functional units like IP_3 receptor (IP_3R) or SERCA pump could lead to different regulation of $[Ca^{2+}]_P$ by anoctamins.

The study of subcellular localization of these different anoctamins showed that some ANOs are localized in the PM and others in intracellular membranes (i.e. endoplasmic reticulum membrane). In HeLa cells overexpressing different ANOs, ANO1 and -6 were found expressed in the PM, whether ANO4, -5, -7, -8, -9, and -10 were found to be in intracellular membranes rather than in the PM. These results indicated that the facilitating or depression of $[Ca^{2+}]_P$ by different ANOs could not be simply explained by localization of ANOs in the PM or ER.

The next step was to address the co-localization of already known Ca^{2+} signaling components, like IP_3R and SERCA pump, with anoctamins. These two proteins are localized in different functional units of Ca^{2+} signaling: IP_3R is responsible for Ca^{2+}

store release and SERCA pump is responsible for Ca^{2+} store input. ANO4 decreases ATP-induced Ca^{2+} signaling and was found to be co-localized with SERCA pump, leading to a decrease in cytosolic [Ca^{2+}]. On the contrary, ANO1, that increases this signaling, was found to be co-localized with IP_3R, channel responsible for Ca^{2+} store release, therefore, an increase in cytosolic [Ca^{2+}] was verified.

Another important observation is that IP_3R showed a distributed localization, close to the PM when ANO1 was overexpressed. ANO4 overexpression did not elicit the same effect.

Taken together, these observations lead to the conclusion that anoctamins regulate Ca^{2+} signaling in different cellular compartments. Furthermore, this suggests that the ER might be tethered to the PM by ANO1, like Jin *et al.* disclosed[37].

5.3 ANOs are organized in Lipid Rafts

The co-localization of ANO1 with IP_3R confirmed the results from Jin *et al.*[37]. In this study it was implicated that ANO1 is localized in lipid rafts, therefore, we analysed whether our PM-GCaMP2 was expressed in these cellular compartments.

Lipid rafts consist in a plasma membrane compartmentalization, made up by cholesterol and proteins like caveolin, or Scp2, a cholesterol transporter important for remodelling of lipid rafts[37].

Surprisingly, when these components of the membrane were disrupted with Filipin, mock and overexpressing ANO4 cells had an enhanced ATP-induced $[Ca^{2+}]_P$ whether ANO1 overexpression had no effect on the ATP-induced changes of $[Ca^{2+}]_P$. This observation could be explained by the hypothesis that the disruption of lipid rafts leads to a loss of ANO1/IP_3R interaction[37], and therefore, a loss of compartmentalized GCaMP2 Ca^{2+} signaling, resulting in an increased non-specific signaling.

After rafts disruption, the change of $[Ca^{2+}]_P$ was no more dependent of ANOs overexpression. This observation may be explained by the existence of more free purinergic receptors on the PM and an enhanced access of the IP_3R. To reach a clear conclusion, more experiments are required.

In conclusion the probe PM-GCaMP2 used was likely expressed in lipid rafts associated with ANO1. These results corroborated the prediction that Ca^{2+} signaling is effectively targeted by anoctamins.

5.4 ANO10 supports ATP-induced Ca^{2+} signaling in intestinal Jejunum Crypts and renal Proximal Tubules

Intestinal Jejunum Crypts and renal Proximal Tubules are responsible for at least a fractional calcium absorption[50,51]. According to our experimental read out ANO10 was found to be expressed in these two kinds of epithelial cells, and we observed that apical ATP-induced Ca^{2+} store release and influx were largely impaired in ANO10 knockout animals, compared to wild-type. This last data suggests the idea that ANO10 supports apical ATP-induced Ca^{2+} signaling in Jejunum Crypts and Proximal Tubules, but not when induced by CCH in the basolateral side (seen in Jejunum Crypts).

The mechanism by which Ca^{2+} signaling regulation works is not fully understood yet, but this work proposes that anoctamins act as counter ion channels or as ER tethering proteins.

1. ANO5 and ANO10 might be localized in the ER membrane, functioning as counter ion channels, and facilitating Ca^{2+} store release (Fig. 23 A). The counter ion channel function was indicated by the experiments showing that the inhibitors, which block Cl^- conductance of anoctamins, prevented the effect of ANOs on $[Ca^{2+}]_P$;
2. Localization of ANO1 to IP_3R tethers the ER to lipid rafts of the PM, compartmentalizing and facilitating $[Ca^{2+}]_P$ changes (Fig. 23 B). This results in a proximity of IP_3Rs to the G protein-coupled receptors (P2Y) giving rise to an increased Ca^{2+} store release;
3. When localized close to SERCA pumps in the ER, e.g. ANO4, the Ca^{2+} signaling close to the PM decreased owing to a counter ion channels function (Fig. 23 C);
4. Or even in an opposite tethering fashion, where the ER is tethered to different cellular compartments besides the PM (Fig. 23 D). This results in a bigger distance between IP_3Rs in the ER with the PM lipid rafts, where the G protein-coupled receptors are, resulting in a decreased Ca^{2+} store release.

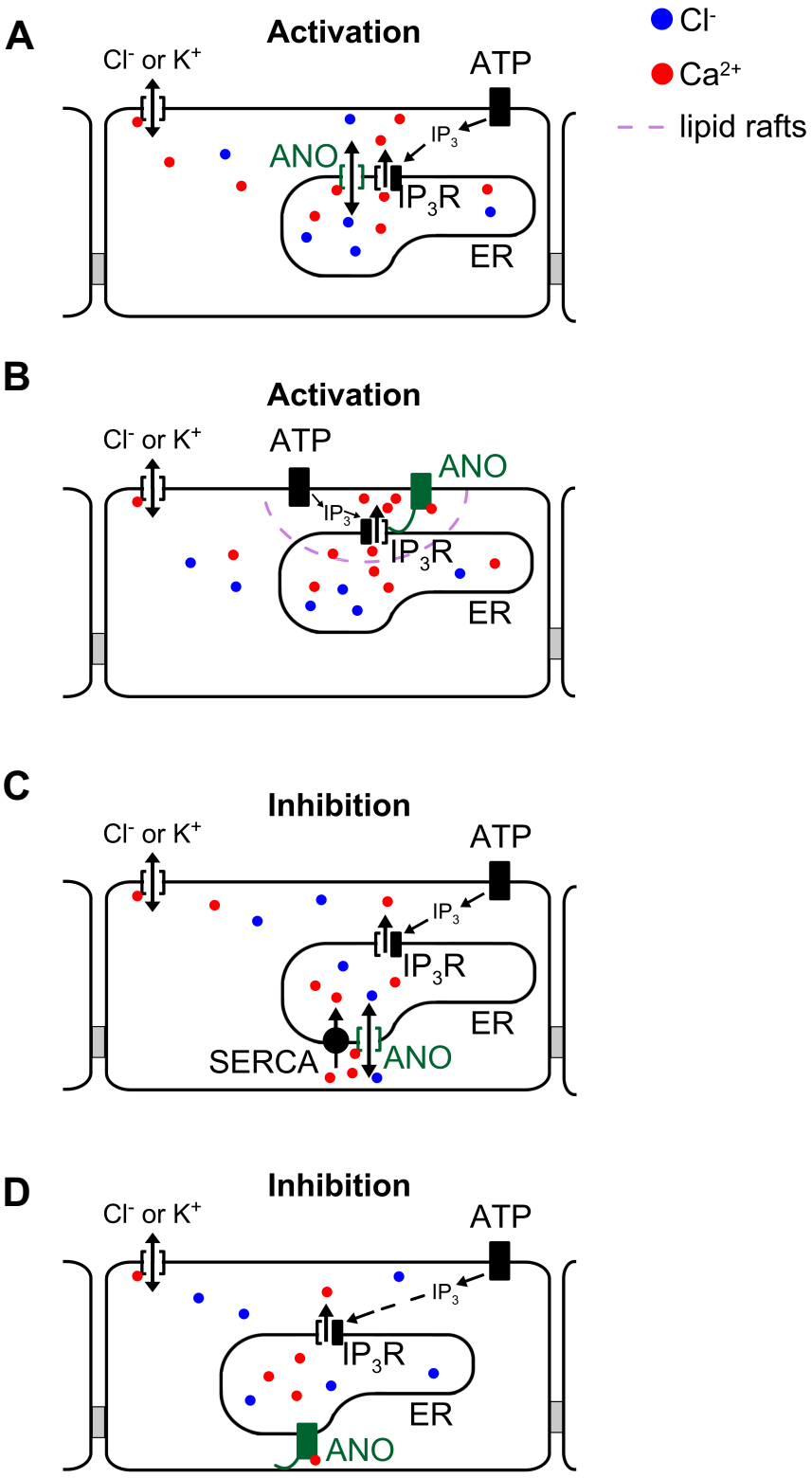

Figure 23. Anoctamins regulate Ca^{2+} signaling, by acting as counter ion channel or by tethering the ER to the PM or other cellular compartments. (A) ANOs might be localized in the ER membrane, functioning as counter ion channels, and facilitating Ca^{2+} store release by IP_3R; **(B)** ANOs can interact with IP_3R tethering the ER to lipid rafts of the PM, compartmentalizing and facilitating $[Ca^{2+}]_P$ changes; **(C)** ANOs might be localized close to SERCA pumps in the ER and decrease Ca^{2+} signaling close to the PM owing to a counter ion channels function; or even **(D)** in an opposite tethering fashion, where the ER is tethered to different cellular compartments besides the PM resulting in a inhibition of Ca^{2+} store release.

6. Future Perspectives

The more this concept of anoctamin-dependent tethering to Ca^{2+} signaling compartments and different target proteins is supported, the more the diversity of function, localization and disease relationships is understood. Different kinds of tissues, with different endogenous expression of the TMEM16 family proteins may explain the whole diversity of Ca^{2+}-related disorders.

The results described here, together with data in the literature, are incentives to further understand this specialized, localized and time-depended Ca^{2+} signaling, but also to find the right tools to elucidate this hidden regulation.

Endogenous protein studies would be very useful in order to reduce the problems related with the plasmid uptake variance, which are characteristic of the over-expressing systems. Since the use of the PM targeted probe, GCaMP2, enlightened our concept, using this indicator to generate fusion proteins with different targeted proteins, like Ora1, TRP, or even the SERCA pump, may solve the problem of different Ca^{2+} compartmentalization. Even an animal model that endogenously expresses this probe could be generated, to support the study of this regulation.

An ER tracker and PM lipid marker live stain, with high resolution confocal images, would be an improvement to the study of different localizations of anoctamins. In fact, the exciting expectations that ER patterns would change with a different expression of anoctamins, would be a great finding.

A lot about ANO1 (which increases Ca^{2+} signaling in lipid rafts) is already known, but what about ANO4 or ANO9, which have been found to function in an opposite fashion yet their exact role is still unclear?

How this ANO/protein interaction and cross-talking work are still unclear, but it surely deserves more investigation.

7. References

1. Berridge, M. J., Lipp, P. & Bootman, M. D. The versatility and universality of calcium signalling. *Nature Reviews Molecular Cell Biology* **1,** 11–21 (2000).
2. Schreiber, R. Ca2+ signaling, intracellular pH and cell volume in cell proliferation. *J. Membr. Biol.* **205,** 129–137 (2005).
3. Mikoshiba, K. IP3 receptor/Ca2+ channel: from discovery to new signaling concepts. *Journal of Neurochemistry* **102,** 1426–1446 (2007).
4. Wang, Y., Deng, X., Hewavitharana, T., Soboloff, J. & Gill, D. L. Stim, ORAI and TRPC channels in the control of calcium entry signals in smooth muscle. *Clin. Exp. Pharmacol. Physiol.* **35,** 1127–1133 (2008).
5. Pozzan, T., Rizzuto, R., Volpe, P. & Meldolesi, J. Molecular and cellular physiology of intracellular calcium stores. *Physiological Reviews* **74,** 595–636 (1994).
6. Blaustein, M. P. & Lederer, W. J. Sodium/calcium exchange: its physiological implications. *Physiological Reviews* **79,** 763–854 (1999).
7. Hartzell, C., Putzier, I. & Arreola, J. Calcium-activated chloride channels. *Annu. Rev. Physiol.* **67,** 719–758 (2005).
8. Ferrera, L., Caputo, A. & Galietta, L. J. V. TMEM16A Protein: A New Identity for Ca2+-Dependent Cl- Channels. *Physiology* **25,** 357–363 (2010).
9. Tarran, R. *et al.* Regulation of murine airway surface liquid volume by CFTR and Ca2+-activated Cl- conductances. *J. Gen. Physiol.* **120,** 407–418 (2002).
10. Mall, M. *et al.* Modulation of Ca2+-Activated Cl− Secretion by Basolateral K+ Channels in Human Normal and Cystic Fibrosis Airway Epithelia. *Pediatr Res* **53,** 608–618 (2003).
11. Grubb, B. R. & Gabriel, S. E. Intestinal physiology and pathology in gene-targeted mouse models of cystic fibrosis. *American Journal of Physiology - Gastrointestinal and Liver Physiology* **273,** G258–G266 (1997).
12. Wagner, J. A. *et al.* Activation of chloride channels in normal and cystic fibrosis airway epithelial cells by multifunctional calcium/calmodulin-dependent protein kinase. *Nature* **349,** 793–796 (1991).
13. Kunzelmann, K. *et al.* Role of the Ca2+-activated Cl- channels bestrophin and

anoctamin in epithelial cells. *Biological Chemistry* **392,** 1–10 (2011).

14. Stephan, A. B. *et al.* ANO2 is the cilial calcium-activated chloride channel that may mediate olfactory amplification. *Proceedings of the National Academy of Sciences of the United States of America* **106,** 11776–11781 (2009).
15. Large, W. A. & Wang, Q. Characteristics and physiological role of the Ca(2+)-activated Cl- conductance in smooth muscle. *American journal of physiology. Cell physiology* **271,** C435–C454 (1996).
16. Duan, D. Phenomics of cardiac chloride channels: the systematic study of chloride channel function in the heart. *The Journal of Physiology* **587,** 2163–2177 (2009).
17. Kawano, S., Hirayama, Y. & Hiraoka, M. Activation mechanism of Ca(2+)-sensitive transient outward current in rabbit ventricular myocytes. *The Journal of Physiology* **486 (Pt 3),** 593–604 (1995).
18. Frings, S., Reuter, D. & Kleene, S. J. Neuronal Ca2+ -activated Cl- channels--homing in on an elusive channel species. *Prog. Neurobiol.* **60,** 247–289 (2000).
19. Runft, L. L., Watras, J. & Jaffe, L. A. Calcium release at fertilization of Xenopus eggs requires type I IP(3) receptors, but not SH2 domain-mediated activation of PLCgamma or G(q)-mediated activation of PLCbeta. *Dev. Biol.* **214,** 399–411 (1999).
20. Liu, B. *et al.* The acute nociceptive signals induced by bradykinin in rat sensory neurons are mediated by inhibition of M-type K+ channels and activation of Ca2+-activated Cl– channels. *Journal of Clinical Investigation* **120,** 1240–1252 (2010).
21. Eggermont, J. Calcium-activated Chloride Channels: (Un)known, (Un)loved? *Proceedings of the American Thoracic Society* **1,** 22–27 (2004).
22. Yang, Y. D. *et al.* TMEM16A confers receptor-activated calcium-dependent chloride conductance. *Nature* **455,** 1210–1215 (2008).
23. Schroeder, B. C., Cheng, T., Jan, Y. N. & Jan, L. Y. Expression Cloning of TMEM16A as a Calcium-Activated Chloride Channel Subunit. *Cell* **134,** 1019–1029 (2008).
24. Caputo, A. *et al.* TMEM16A, a membrane protein associated with calcium-dependent chloride channel activity. *Science* **322,** 590–594 (2008).
25. Kunzelmann, K., Milenkovic, V. M., Spitzner, M., Soria, R. B. & Schreiber, R.

Calcium-dependent chloride conductance in epithelia: is there a contribution by Bestrophin? *Pflügers Archiv - European Journal of Physiology* **454,** 879–889 (2007).

26. Kunzelmann, K. *et al.* Anoctamins. *Pflügers Archiv - European Journal of Physiology* **462,** 195–208 (2011).
27. Pedemonte, N. & Galietta, L. J. V. Structure and Function of TMEM16 Proteins (Anoctamins). *Physiological Reviews* **94,** 419–459 (2014).
28. Brunner, J. D., Lim, N. K., Schenck, S., Duerst, A. & Dutzler, R. X-ray structure of a calcium-activated TMEM16 lipid scramblase. *Nature* **516,** 207–212 (2014).
29. Wasserman, M. A. & Mukherjee, A. Regional differences in the reactivity of guinea-pig airways. *Pulm Pharmacol* **1,** 125–131 (1988).
30. Dho, S., Stewart, K. & Foskett, J. K. Purinergic receptor activation of Cl- secretion in T84 cells. *American journal of physiology. Cell physiology* **262,** C67–C74 (1992).
31. Barrett, K. E. & Keely, S. J. Chloride secretion by the intestinal epithelium: molecular basis and regulatory aspects. *Annu. Rev. Physiol.* **62,** 535–572 (2000).
32. Schreiber, R. *et al.* Anoctamins support calcium-dependent chloride secretion by facilitating calcium signaling in adult mouse intestine. *Pflügers Archiv - European Journal of Physiology* **467,** 1203–1213 (2014).
33. Yang, H. *et al.* TMEM16F Forms a Ca2+-Activated Cation Channel Required for Lipid Scrambling in Platelets during Blood Coagulation. *Cell* **151,** 111–122 (2012).
34. Ousingsawat, J. *et al.* Anoctamin-6 Controls Bone Mineralization by Activating the Calcium Transporter NCX1. *Journal of Biological Chemistry* **290,** 6270–6280 (2015).
35. Stefan, C. J., Manford, A. G. & Emr, S. D. ER–PM connections: sites of information transfer and inter-organelle communication. *Current Opinion in Cell Biology* 1–9 (2013). doi:10.1016/j.ceb.2013.02.020
36. Wolf, W. *et al.* Yeast Ist2 Recruits the Endoplasmic Reticulum to the Plasma Membrane and Creates a Ribosome-Free Membrane Microcompartment. *PLoS ONE* **7,** e39703–13 (2012).
37. Jin, X., Shah, S., Du, X., Zhang, H. & Gamper, N. Activation of Ca 2+-activated Cl −channel ANO1 by localized Ca 2+signals. *The Journal of Physiology* n/a–

n/a (2014). doi:10.1113/jphysiol.2014.275107

38. Perez-Cornejo, P. *et al.* Anoctamin 1 (Tmem16A) Ca2+-activated chloride channel stoichiometrically interacts with an ezrin-radixin-moesin network. *Proceedings of the National Academy of Sciences of the United States of America* **109,** 10376–10381 (2012).
39. Tallini, Y. N. *et al.* Imaging cellular signals in the heart in vivo: Cardiac expression of the high-signal Ca2+ indicator GCaMP2. *Proceedings of the National Academy of Sciences of the United States of America* **103,** 4753–4758 (2006).
40. Su, S. *et al.* Genetically encoded calcium indicator illuminates calcium dynamics in primary cilia. *Nat. Methods* **10,** 1105–1107 (2013).
41. Watts, S. D., Suchland, K. L., Amara, S. G. & Ingram, S. L. A Sensitive Membrane-Targeted Biosensor for Monitoring Changes in Intracellular Chloride in Neuronal Processes. *PLoS ONE* **7,** e35373–9 (2012).
42. Landry, J. J. M. *et al.* The genomic and transcriptomic landscape of a HeLa cell line. *G3 (Bethesda)* **3,** 1213–1224 (2013).
43. Hsu, S. *et al.* Genetic characteristics of the HeLa cell. *Science* **191,** 392–394 (1976).
44. Grynkiewicz, G., Poenie, M. & Tsien, R. Y. A new generation of Ca2+ indicators with greatly improved fluorescence properties. *Journal of Biological Chemistry* **260,** 3440–3450 (1985).
45. Ni, Y.-L., Kuan, A.-S. & Chen, T.-Y. Activation and inhibition of TMEM16A calcium-activated chloride channels. *PLoS ONE* **9,** e86734 (2014).
46. Namkung, W., Phuan, P. W. & Verkman, A. S. TMEM16A Inhibitors Reveal TMEM16A as a Minor Component of Calcium-activated Chloride Channel Conductance in Airway and Intestinal Epithelial Cells. *Journal of Biological Chemistry* **286,** 2365–2374 (2011).
47. Bootman, M. D. *et al.* Calcium signalling—an overview. *Seminars in Cell & Developmental Biology* **12,** 3–10 (2001).
48. Awasthi-Kalia, M., Schnetkamp, P. P. & Deans, J. P. Differential effects of filipin and methyl-beta-cyclodextrin on B cell receptor signaling. *Biochemical and Biophysical Research Communications* **287,** 77–82 (2001).
49. Tian, Y., Schreiber, R. & Kunzelmann, K. Anoctamins are a family of Ca2+-activated Cl- channels. *Journal of Cell Science* **125,** 4991–4998 (2012).

50. Ullrich, K. J., Rumrich, G. & Klöss, S. Active Ca2+ reabsorption in the proximal tubule of the rat kidney. Dependence on sodium- and buffer transport. *Pflügers Archiv - European Journal of Physiology* **364,** 223–228 (1976).

51. Wasserman, R. H. Vitamin D and the dual processes of intestinal calcium absorption. *J. Nutr.* **134,** 3137–3139 (2004).

Appendices

Appendix I – cDNA and siRNA

Table I.1. Accession Nº. and base pairs (bp) of the plasmids used.

Target	Accession No.	Size (bp)
ANO1	NM_178642.4	**75**
ANO4	NM_178773.4	**93**
ANO5	NM_177694.5	**71**
ANO6	NM_175344.3	**81**
ANO7	NM_207031.1	**62**
ANO8	XM_889480.2	**69**
ANO9	NM_178381.3	**60**
ANO10	NM_133979.2	**61**
GAPDH	NM_001289745	**98**
sihANO6	NM_001142678	**25**
sihANO10	NM_018075AK131223.1	**21**

Appendix II – Primers and RT-PCR

Table II.1. Pair list of Primers used for RT-PCR designed with Probe Finder Software from Roche Applied Science (www.roche-applied-science.com).

Template	Sequence	Size (bp)
ANO1	CGA CTA CGT GTA CAT TTT CCG GAT TCC GAT GTC TTT GGC TC	**445**
ANO2	GTC TCA AGA TGC CAG GTC CC CTG CCT CCT GCT TTG ATC TC	**553**
ANO3	CTT CCC TCT TCC AGT CAA C AAA CAT GAT ATC GGG GCT TG	**461**
ANO4	CGG AAG ATT TAC AGG ACA CCC GAT AAC AGA GAG AAT TCC AAT GC	**503**
ANO5	GAA TGG GAC CTG GTG GAC GAG TTT GTC CGA GCT TTT CG	**713**
ANO6	GGA GTT TTG GAA GCG ACG C GTA TTT CTG GAT TGG GTC TG	**325**
ANO7	CTC GGG AGT GAC AAC CAG G CAA AGT GGG CAC ATC TCG AAG	**470**
ANO8	GGA GGA CCA GCC AAT CAT C TCC ATG TCA TTG AGC CAG	**705**
ANO9	GCA GCC AGT TGA TGA AAT C GCT GCG TAG GTA GGA GTG C	**472**
ANO10	GTG AAG AGG AAG GTG CAG G GCC ACT GCG AAA CTG AGA AG	**769**

Table II.2. Standard RT-PCR program.

Target gene	Temperature (ºC)	Time	Number of cycles
ANO1-10	95ºC 95ºC 57ºC 72ºC 72ºC 8ºC	2 min 30 sec 60 sec 1 min 7 min hold	**30x**

Appendix III – Animal models Genotyping

Table III.1. Standard PCR programs for Villin $Cre^{+}/ANO10^{loxp/loxp}$ and $Pax8Cre^{+}/ANO10^{loxp/loxp}$ Genotyping.

Target gene	Temperature (ºC)	Time	Number of cycles
Villin Cre	94ºC	3 min	**35x**
	94ºC	30 sec	
	64ºC	60 sec	
	72ºC	1,5 min	
	72ºC	2 min	
	8ºC	hold	
Pax8Cre	94ºC	3 min	**35x**
	94ºC	30 sec	
	58ºC	60 sec	
	72ºC	1,5 min	
	72ºC	3 min	
	8ºC	hold	
ANO10 flox	95ºC	5 min	**35x**
	95ºC	30 sec	
	56ºC	30 sec	
	72ºC	1 min	
	72ºC	7 min	
	8ºC	hold	

Table III.2. Genotyping Primers.

Target gene	Primers (5' → 3')	Size (bp)
Villin Cre	**$oIMR_{1878}$** GTG TGG GAC AGA GAA CAA ACC **$oIMR_{1879}$** ACA TCT TCA GGT TCT GCG GG	**1 100**
Pax8Cre	**PrimerA** AAT TTA CTG ACC GTA CAC **PrimerB** AAT CGC CAT CTT CCA GCA G	**1 024**
ANO10 flox	**wt – Inst/E7as** CCA ACA CTT TCA GAA CGA GAT G **flox – Inst/con1as** GCA TCA ATT CTC TAG AGC TCG (**Inst** CTC ATT TGC AAC ACT TCC C)	**303** **450**

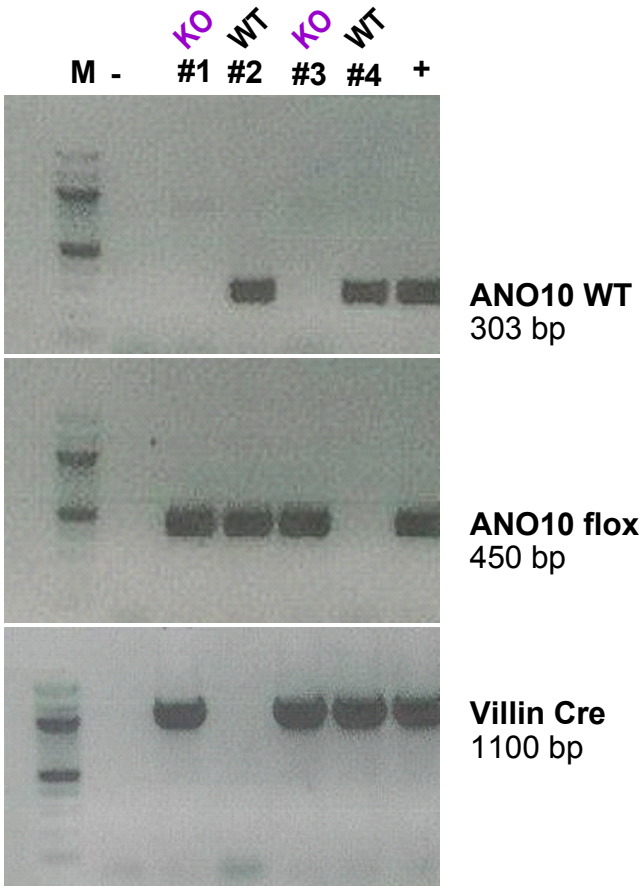

Figure III.1. Genotype results for Villin Cre^{+}/$ANO10^{loxp/loxp}$ mice.

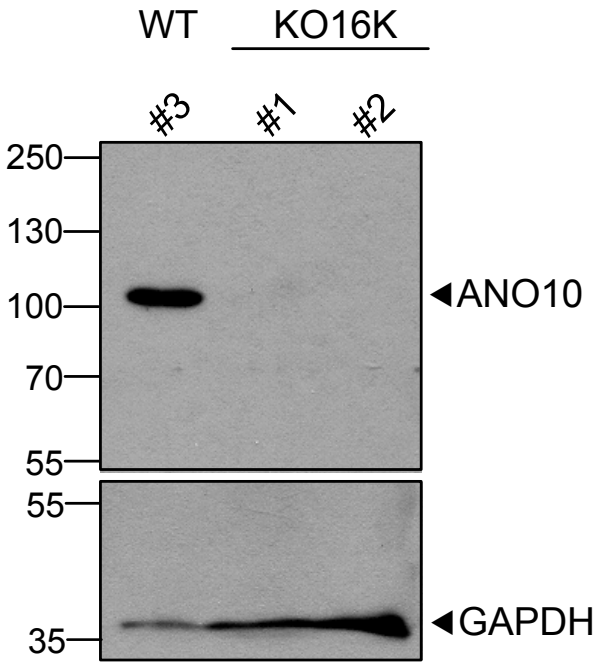

- Input 75 μg protein
- 1:1000 Rabbit anti ANO10 (Aviva) in 3%NFM/PBST, O/N 4 °C
- 1:3000 Rabbit anti GAPDH (Santacruz) in 5%NFM/TBST, O/N 4°C

Figure III.2. Genotype confirmed by *Western Blot* for Villin Cre^{+}/$ANO10^{loxp/loxp}$ mice.

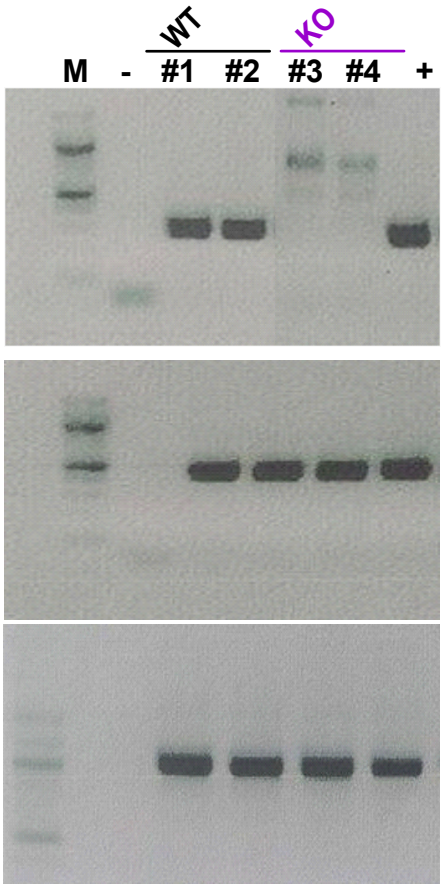

Figure III.3. Genotype results for Pax8Cre^{+}/ANO10$^{loxp/loxp}$.

Appendix IV – Fura-2 AM Original tracings

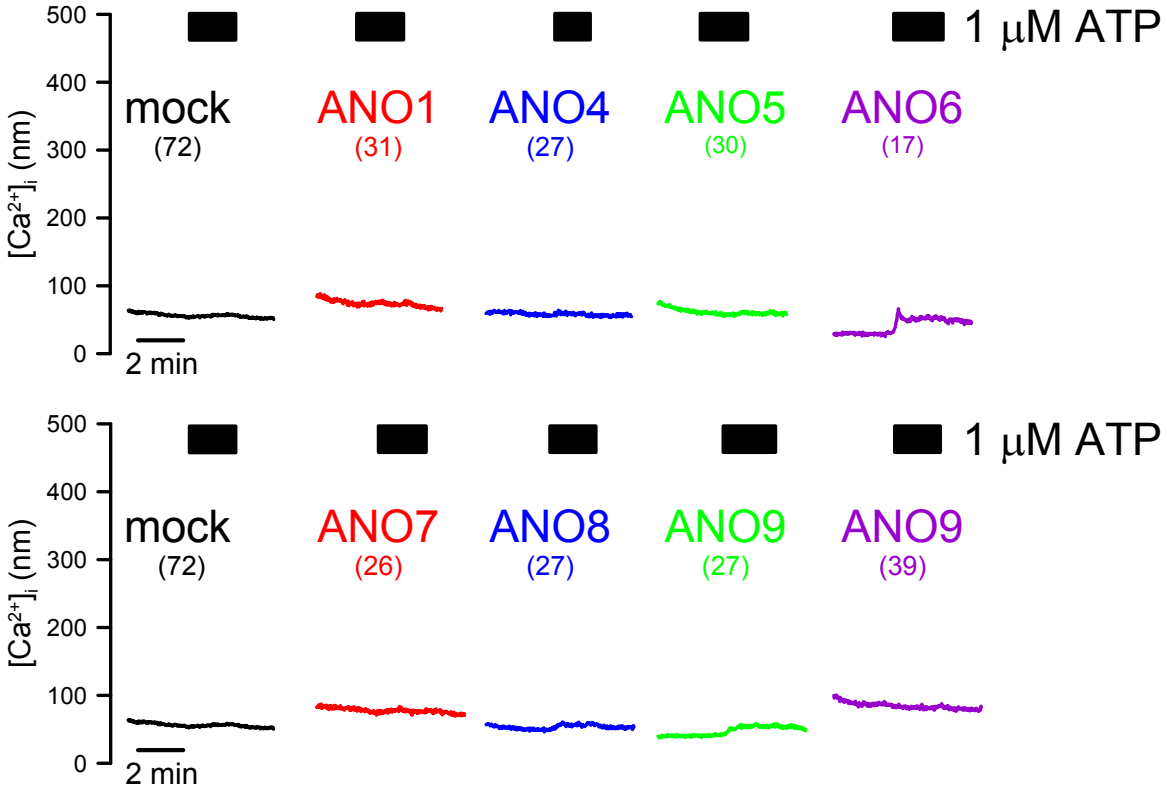

Figure IV.1. Original mean tracing of purinergic 1μM ATP stimulation from HeLa cells co-expressing ANOs and CD8; (n) = number of cells.

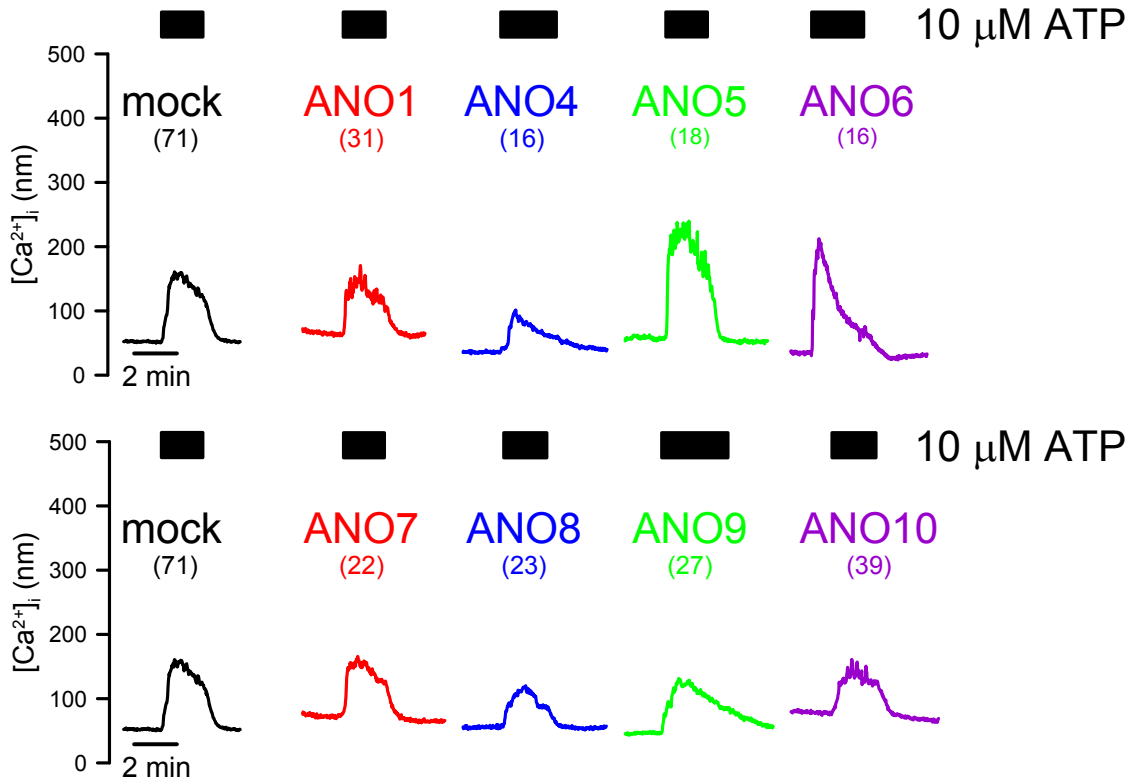

Figure IV.2. Original mean tracing of purinergic 10 µM ATP stimulation from HeLa cells co-expressing ANOs and CD8; (n) = number of cells.

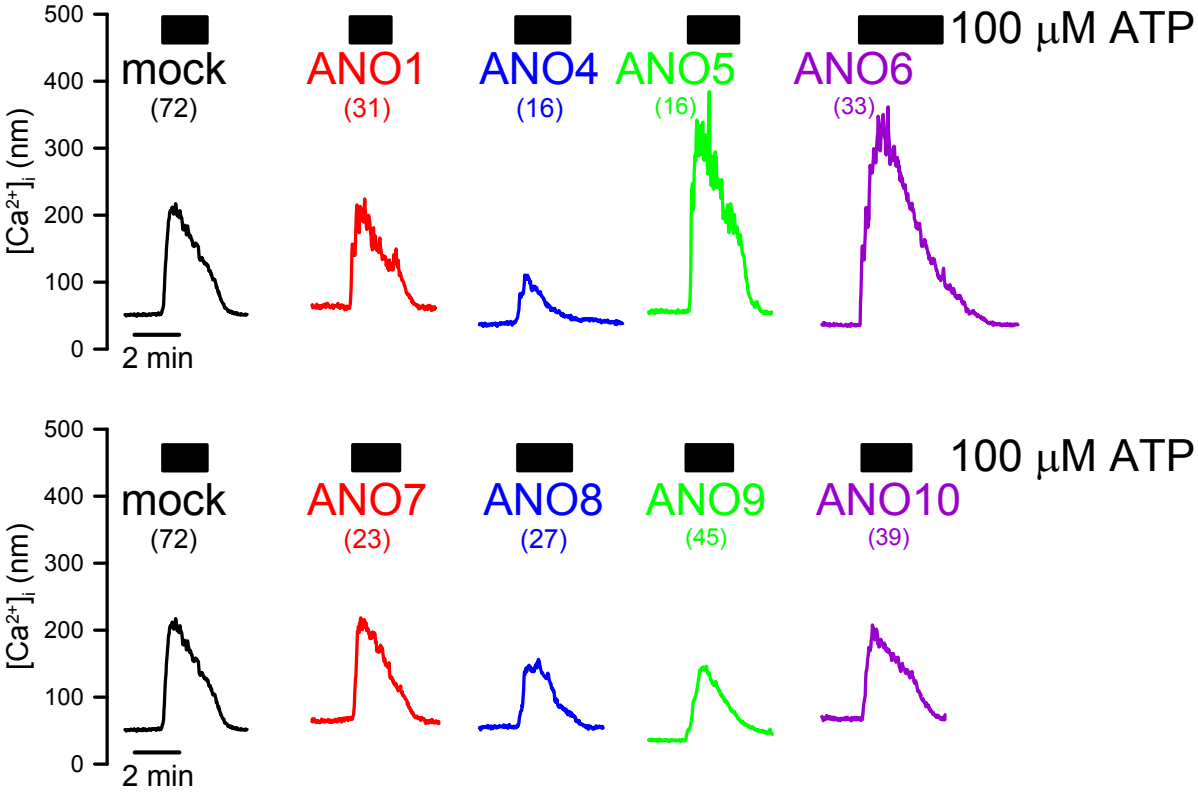

Figure IV.3. Original mean tracing of purinergic 100 µM ATP stimulation from HeLa cells co-expressing ANOs and CD8; (n) = number of cells.

Appendix V – PM- GCaMP2 Original tracings

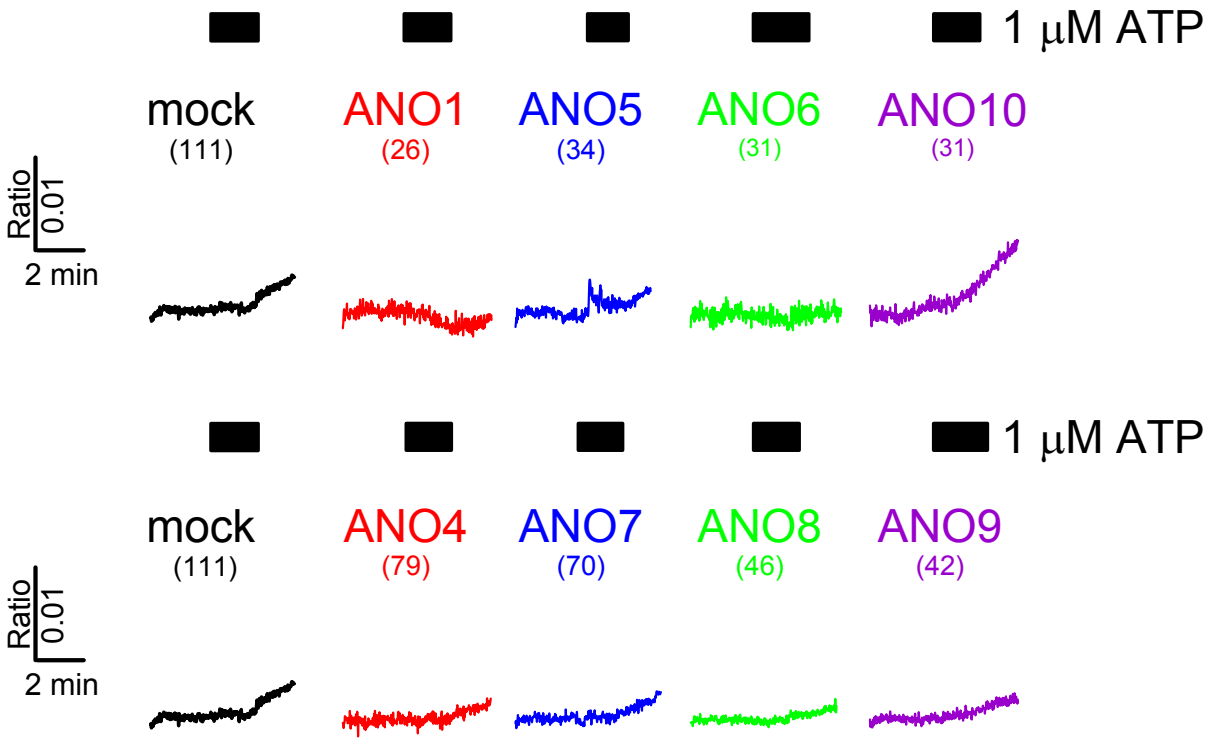

Figure V.1. Original mean tracing of purinergic 1μM ATP stimulation from HeLa cells co-expressing ANOs and GCaMP2; (n) = number of cells.

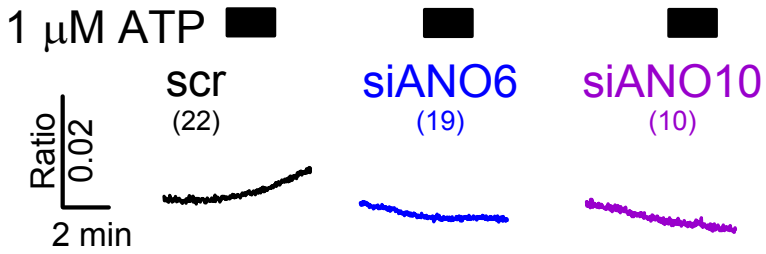

Figure V.2. Original mean tracing of purinergic 1μM ATP stimulation from HeLa cells with PM-GCaMP2 and with whether ANO6 or -10 downregulated; (n) = number of cells.